Synthesis, Characterization and Electrochemical studies of Zeolitic Imidazolate Frameworks (ZIFs) Derived Nano-porous Carbon Based Materials

By

Rabia Saghir

Department of Chemistry

Quaid e Azam University

Islamabad

(2021)

Synthesis, Characterization, and Electrochemical studies of Zeolitic Imidazolate Frameworks (ZIFs) Derived Nano-porous Carbon Based Materials

A dissertation submitted to the Department of Chemistry, Quaid-e-Azam University, Islamabad, in partial fulfillment of the requirements for the degree of

Master of Philosophy

In

Analytical / Inorganic Chemistry

By

Rabia Saghir

Department of Chemistry

Quaid e Azam University

Islamabad

(2021)

Acknowledgements

All the praises are attributed to almighty Allah, the compassionate, the merciful. He is the source of all wisdom, who gave me the strength to work for this thesis. We offer our humblest thank to the Holy prophet (peace be upon him) who is forever a model of guidance and knowledge for humanity.

I would like to express my deep and sincere gratitude to my supervisor **Prof. Dr. Zareen Akhter,** Department of Chemistry, Quaid-e-Azam University, Islamabad and Dr. Naveed Zafar Ali for his inspiring guidance, remarkable suggestions, constructive criticism and kind attitude during my project work. I greatly benefited from their keen scientific insight for solving practical difficulties and the ability to put complex ideas into simple terms. Without their support and guidance, this report could not have been possible.

I would like to thank Prof. Dr. Shahid Hameed, chairman of Department of chemistry providing us an opportunity to work in this department. I would like to acknowledge my friends, seniors and lab fellows for listening, offering me advice and supporting me through this entire process of completing my project.

Rabia saghir


بسم الله الرحمن الرحيم

Author declaration

I hereby declare that I have done all this work myself and has not used any sources or tools other than those specified. Further, I confirm that this work has not been submitted for any other degree.

Rabia Saghir

Abstract

For many past years, metal oraganic frameworks (MOFs) have been promising candidate for hydrogen evolution reaction (HER) and oxygen evolution reaction (OER) due to their high surface area, good porosity and tuneable properties. The benchmark catalysts for hydrogen evolution reaction (HER) and oxygen evolution reaction (OER) are Pt/C and IrO_2 but their high cost, low stability and scarcity has limited their applications. One of the drawback of MOFs is that they have poor conductivity due to presence of organic ligands. In order to overcome the conductivity problem, composite of ZIF (subclass of MOF) is made with GO in the present work. The simple and clean mixing method (sonication and stirring) was used to synthesize zeolitic imidazolate framework (ZIF-67 and ZIF-8), their composite with GO followed by their carbonization in tube furnace. Nanoporous carbon based materials have good electrical conductivity, high surface area and they exhibit excellent chemical and mechanical stability.

The synthesized materials are characterized by XRD, IR, TGA and BET,SEM and EDX. XRD confirms the phase purity and crystallinity, IR confirms the presence of functional group. TGA gives information about thermal stability of materials and BET tells about the surface area. Electrochemical studies of synthesized material were done by using linear sweep voltammetry (LSV), Electrochemical impedence spectroscopy (EIS) and Tafel slope.

Table of contents

List of Figures

List of Tables

List of Abbreviations

CV	Cyclic voltammetry
EIS	Electrochemical impedence spectroscopy
GO	Graphene oxide
HER	Hydrogen evolution reaction
LSV	Linear sweep voltammetry
MOF	Metal organic framework
OER	Oxygen evolution reaction
ORR	Oxygen reduction reaction
OPD	Overpotentially deposited hydrogen
rGO	Reduced graphene oxide
UPD	Underpotentially deposited hydrogen
ZIFs	Zeolitic Imidazolate frameworks

Chapter 1

INTRODUCTION

This chapter gives the short presentation of electrochemical redox reactions, for example, oxygen evolution reaction (OER) and hydrogen evolution reaction (HER) that have brought growing concerns because of their significant jobs in numerous energy cycles, for example, fuel cell, batteries and water electrolysis.

1.1 Energy crisis

With the increasing world's population, there is an increase in energy demand which will be doubled in next two decades. Currently, fossil fuels are the only source to meet this demand. However, fossil fuels have limited sources and they cause many environmental problems. In order to overcome the crisis of fossil fuel depletion and energy demands, it is the need of hour to develop alternative, sustainable, environment friendly, renewable energy resources. Wind and sunlight are the two common sources for energy production but due to unreliability of nature, we cannot fully rely on them. For example, wind power energy is maximum captured in early morning when winds are at peak and for solar power maximum energy is captured during daytime. Similarly, geothermal energy, wave energy, and tidal power are the abundant sources of energy, but they also have a problem that they can be produced in selected areas. Due to these problems researchers move towards alternative energy conversion methods. In energy conversion, the most important thing is the material of electrode. Nanomaterials show better performance in energy applications due to their remarkable chemical, physical and electrochemical properties.[1]

1.2 Electrochemical reduction reaction

The term redox alludes to various oxidation and reduction reactions. It addresses electrochemical cycles including electron move to or from a molecule or ion. Such

reactions occur with the help of external source. Oxidation and reduction reaction differ in the oxidation state that occurs in ions, molecules or atoms during electrochemical reaction. HER and OER reactions are the premise of different energy storage and transformation devices. The expanding measure of changing environmentally friendly power made such transformation responses as alluring device for energy storage.To advance the practical utilizations of energy gadgets, proficient electrocatalysts for OER, ORR and HER are needed to bring down the energy hindrance and improve the effectiveness. For the electrolysis, the electrocatalysts ought to have quick electron and mass transport regions, and give plentiful regions to surface reaction. Along these lines, such encouraging candidates are required that have high electrical conductivity and tunable porous design to construct exceptionally dynamic oxygen/hydrogen electrocatalysts.[3]

Up until now, dynamic materials for oxidation and reduction electrocatalysis are noble metals and their mixtures (Pt for ORR and HER) and (IrO2 for OER). Because of restricted stores and significant expense of such materials, non-noble metals were researched as choices for electrocatalysis. For these electrocatalysts with metal-based active sites, carbon materials can be utilized as multi-functional backings to upgrade charge and mass transport. In the past decade, carbon itself act as active materials for HER, OER, ORR and for other electrocatalysis.[4]

1.3 Metal-organic frameworks (MOFs)

Metal-Organic Frameworks comprising of metal ions facilitated to natural ligands to frame one, two or three dimensional structures. They are frequently permeable. The natural ligands are frequently alluded as linkers. A metal-organic system is a coordination network that comprise of natural ligands with likely voids. Sometimes, pores are foemed during evacuation of visitor particles like solvents and could be loaded up with different mixtures. Due to this property MOFs have various applications like they store gases e.g hydrogen and carbon dioxide. Other utilization of MOFs is in gas separation and in catalysis. High porosity and crystallinity of MOFs separate them from traditional co-ordination compounds.[5]

Those ligands that have aromatic part are mostly preferred because they provide rigid framework. Carboxylate, cyanides, phosphates and nitrogen containing compounds

such as imidazole's and pyridines are the most common functional groups of organic ligands that coordinate with metal ions. Both the metal ion and organic ligand can be changed for tuning of porosity and other properties while other conventional inorganic materials do not have this property.[6] The conventional and simple method for MOF synthesis is solvothermal method. This method can be easily processed and controlled.

1.3 MOFs Synthesis

MOF can be synthesized by different methods. The most conventional and simple method for MOF synthesis is solvothermal method. This method can be easily processed. Methods of MOF synthesis are given below.

1.3.1.1 Solvothermal method

In this method, reactants are mixed in the presence of suitable solvent and transferred to a Teflon lined reactor and heated at elevated temperatures. With the increase in temperature, reactants start to dissolve slowly, and product is obtained in the form of crystals.[7]

1.3.1.2 Microwave assisted synthesis

In this method, reactants and solvent are placed in autoclave and autoclave is placed on microwave unit. The dipole moment of reactant molecules coupled with the oscillating electric field in reaction medium and assist molecular motions which creates high temperature environment for reaction.[8]

1.3.1.3 Sonochemical method

In this method, Pyrex glass reactor is placed in sonicator. The reaction mixture and solvent are placed in reactor. Upon sonication, bubbles are formed in solution due to creation of high temperature and pressure. In this way, reactants start reacting with each other that results into the formation of MOFs.[9]

1.3.1.4 Electrochemical synthesis

In this method, metal ion act as an anode and the same metal bulk is used as a cathode. Ligand which is dissolved in a solvent act as a conducting medium. The anodic metal ion reacts with the ligand molecules and generate H_2 gas.[10]

1.3.1.5 Mechanochemical synthesis

This method involves the mechanical grinding of reactants which results in bond breaking in the molecules and chemical reaction takes place. This synthesis takes place in the absence of solvents. Sometimes smaller amount of solvent is added at the starting point which is called liquid assisted grinding.[11]

1.4 Zeolitic-Imidazolate Frameworks (ZIFs)

Zeolitic-imidazolate Frameworks (ZIFs) are a class of metal-organic frameworks (MOFs) that are isomorphic with zeolites. ZIFs are made out of tetrahedrally-coordinated transition metal ions (for example Fe, Co, Cu, Zn) associated by imidazolate linkers. In ZIFs, the metal-imidazole-metal angle resembles Si-O-Si point in zeolites so ZIFs have zeolite like topology. They are chemically stable, and they show amazing stability to thermal changes because of their vigorous porosity.[12]

1.4.1 ZIFs Synthesis

ZIFs are made by solvothermal or hydrothermal methods.

1.4.1.1 Solvothermal method

In this method, reactants are mixed in the presence of suitable solvent and transferred to a Teflon lined reactor which is heated at a temperature of 100-200 ^{0} C. With the increase of temperature, the reactants dissolve slowly and react above the boiling point of the solvent at autogenous pressure. The product is obtained in the form of crystals which can be analyzed by single crystal XRD. By using this method, one have a control over the size, shape distribution, and crystallinity of material. These properties can be changed by altering the experimental parameters, including reaction temperature, reaction time, solvent type and precursor type.

1.4.1.2 Hydrothermal method

Hydrothermal method is used to synthesize single crystals. The reaction is carried out in an autoclave that has teflon lining inside and steel covering outside. Reactants along with the solvent are added in teflon lined reactor. A temperature gradient is set up between the opposite ends of the growth chamber. Hydrothermal method have the advantage over the other types of method that it has ability to create crystalline phases. Also, the materials that have high vapor. pressure near their boiling points can be grown

by hydrothermal method. This method produces large amount of crystals with controllable composition. There are many methods that can be applied in hydrothermal technique.[13]

1. Temperature-difference method

2. Temperature-reduction method

3. Metastable phase method

1.4.3 Non-Solvent based synthesis

(a) Solvent minimization method

Although the synthesis of ZIFs in an aqueous-based system is environment friendly and do not produces harmless substances as compared to organic solvents, but still there are some problems like there is excessive waste of solvent during washing as well as much use of imidazole sources. Due to this reason, solvent minimization method is applied. In this method, metal salts and organic ligands are placed in Teflon cups surrounded by water vapor (or organic solvent steam) at 120^{0} C for 24 h.[14]

(b) *Mechanochemical synthesis*

Mechanochemical method is also used to synthesize materials with no harmful side products. Therefore, this method is also adopted for the synthesis of ZIFs. The mechanochemical synthesis involves the mechanical grinding of reactants which results in bond breaking in molecules and chemical reaction takes place simultaneously in the absence of the solvent. Sometimes smaller amount of liquid is added at the starting point which is called liquid assisted method.[15]

1.5 Difference between ZIFs and MOFs

ZIFs are the subclass of MOFs. Their structure is more restricted because they have imidazole-based organic ligands while MOFs have variety of organic ligands that can attach with metal ion. Secondly, ZIFs have zeolite like structure that's why they are chemically and thermally more stable than MOFs and they can be operated at wide range of temperatures. ZIFs show hydrophobic properties due to which they are more stable in water`while MOFs are less stable in water because of presence of metal-oxygen bonds. Because of this property, ZIFs absorb CO_2 more efficiently and

effectively as compared to MOFs as they absorb moisture alongwith CO_2 and thus shows less selectivity for CO_2.

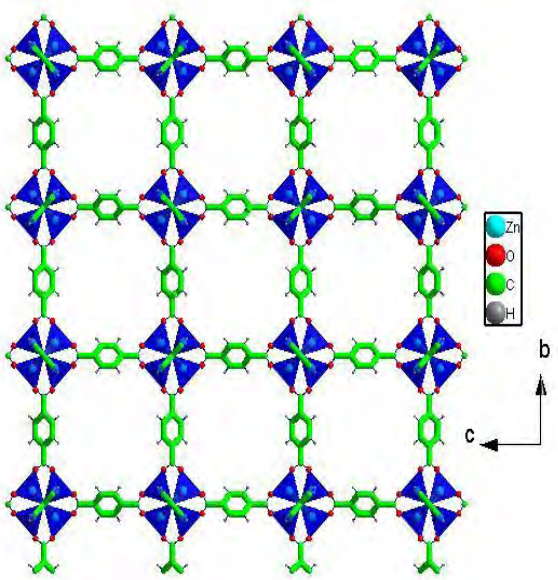

Figure 1.1 General structure of Zeolitic imidazolate framework

1.6 Hydrogen Evolution Reaction (HER)

Hydrogen evolution reaction (HER) is the most simplest electrocatalytic reaction. A great deal of consideration has been paid to HER in electrochemistry as it was important to numerous electrochemical innovations because of the thought of this response to create hydrogen as a fuel that can possibly supplant fossil-based transportation powers. With the advancement of environmentally friendly power sources, creation of hydrogen turns into an elective method for internal combustion engines and energy units. It is the cathodic reaction in electrochemical water splitting.[16]

HER includes hydrogen adsorption at anode surface and the adsorption energy relies upon the nature of electrode material. There are two kinds of adsorbed hydrogen at surfaces. At some noble metals (Pt, Pd, Ir) a solid hydrogen adsorption happens, this is called underpotentially deposited hydrogen, UPD. Another kind of adsorbed hydrogen is the over potentially deposited hydrogen, OPD. These two sorts of hydrogen exist at the same time on noble metals however just H OPD is associated with the HER. Surface inclusion of H UPD changes with potential from zero to one while that of the H OPD changes starting from one value to another and not really from zero to one.[17].

The HER happens when protons or water undergo reduction at the anode surface. HER requires free active sites at the metal surface for adsorbing hydrogen. HER happens in two step reactions. The first step is known as the Volmer or discharge reaction in which aqueous protons are electrochemically diminished to atomic hydrogen and adsorbed on the metal surface. In the subsequent advance, H_2 is framed, either by a chemical reaction or as an electrochemical reaction. This reaction is known as the Tafel or combination reaction where two atomic hydrogen join to frame molecular hydrogen. In an electrochemical reaction, combination of a proton, an atomic hydrogen, and an electron produces molecular hydrogen. This reaction is known as the Heyrovsky (ion + atom) reaction.[18]

Fig.1.2 represents the mechanism of HER in acidic and alkaline media [19]

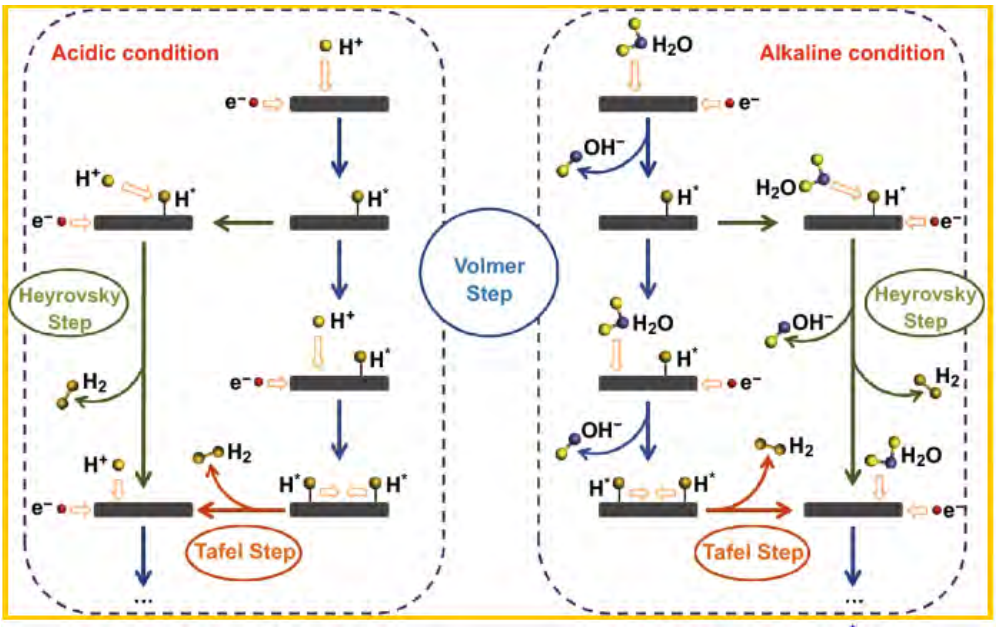

Figure 1.2 Schematic pathway of HER in acidic and alkaline conditions

1.7 Oxygen Evolution Reaction (OER)

Oxygen evolution reaction (OER) is inverse reaction to ORR and is regularly used to couple with different reactions in a few key sustainable power frameworks, like solar cells, metal-air batteries, and electrochemical splitting.

Oxygen evolution reaction (OER) is a process of producing molecular oxygen through chemical reaction, for example, O_2 is produced as a result of oxidation of water during photosynthesis, electrolysis of water produces O_2 and H_2, and there is also evolution of O_2 from oxides and oxoacids. Creating improved catalysts for the OER is the way into the progression of a few sustainable power advances, including sunlight based powers creation and metal-air batteries. Although noble metal oxides, like ruthenium and iridium oxides show the best OER activity, but their shortage and significant expenses has limited their versatile applications. As of now, the basic test is to investigate elective non-precious metal catalysts for the advancement of the kinetically sluggish OER.[20] Fig.1.3 represents the mechanism of OER in both acidic and alkaline media.[21]

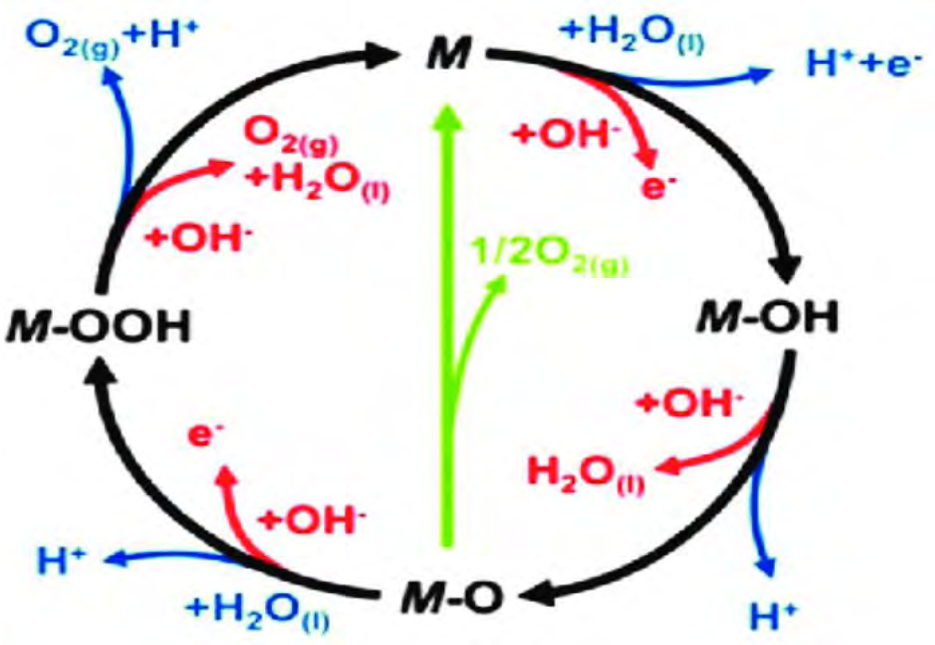

Figure 1.3 OER mechanism in acidic and alkaline medium

1.7.1 Mechanism of OER

OER is one of the crucial cycle including the exchange of four electrons and liable for the more slower kinetics of water splitting process. O*, OOH*, OH* are the primary intermediates saw in the OER. Accordingly, in OER reaction, the M-O bonding has a critical job in stabilizing the reaction intermediates on a superficial level, and that pronouncedly affects the general water splitting effectiveness.

OER system comprises of four-electron/proton transfer steps in both acidic and basic media. The OER is exceptionally pH touchy. Under acidic conditions, water molecules are oxidized, and oxygen molecules are delivered in basic media, hydroxyl groups are oxidized to H_2O and O_2 with the release of electrons.[22]

1.8 Catalysts for HER and OER

1.8.1 Noble metal based electrocatalysts

The noble metals like iridium, ruthenium, rhodium, silver and gold were first utilized for HER and OER but since of their low shortage, they are not reasonable for enormous scope make in labs and industries. Noble metals (like Pt and Pd) and their compounds are as yet utilized as catalysts for HER and OER. The issue is that the shortage and excessive cost of honorable metals builds the expense of these metals. Subsequently, serious examinations have focused in on the advancement of low cost electrode materials in contrast to noble metal-based catalysts. Presently, numerous scientists utilize bimetallic catalyst frameworks, for example, a compound of Pt and 3d square metals like Ni, Cu, Co and Fe. These catalysts have low Pt content and higher catalytic action because of geometric and electronic impacts.

A simple methodology is to decrease the loading of noble metals, like Pt yet to keep up the high action and stability of the catalyst. In past examinations a few strategies have been proposed. One of which is to dope Pt into fine construction to boost the exposure of the active site. Another methodology is to supplant noble metals with relative low cost transition metals.[23]

1.8.2 Non-noble transition metal based electrocatalysts

Despite the fact that the noble metals have shown high catalytic activity for HER and OER, however its significant expense restricts its enormous scope application. Along these lines, analysts are attempting to utilize reasonable, non-noble metal catalysts to

supplant noble metal-based catalysts. Among non-noble metal catalysts Fe, Co, Cu and Ni are the most studied material. Co is earth-bountiful transition metal.The high corrosion resistance and huge amount of Co makes it perhaps the best possible match for HER and OER substrates.

Metal-organic frameworks (MOFs) have been showed up as promising candidate for electrochemical water splitting. MOFs are porous crystalline materials with high surface area. They are framed by metal hubs and natural ligands. MOFs have extraordinary structural characterizations like high porosity, ultrahigh explicit surface area and tunable pore structure. Zeolitic imidazolate systems (ZIFs) are the subclass of MOFs. ZIFs are particularly intriguing on the grounds that they can be utilized as productive permeable carbon-based electrocatalysts. ZIFs have cross-connected three-dimensional network structures, enormous pore volumes and profoundly explicit surface areas. Also, ZIFs have nitrogen atoms within the imidazole groups that go about as electronegative atom which further upgrades the electrolysis cycle.[24]

1.9 Pyrolysis

Pyrolysis is the thermal disintegration of materials at high temperatures in an inert environment. It includes a difference in substance composition. The word pyrolysis comes from Greek phrasing, pyro signifies "fire" and lysis signifies "isolating". Pyrolysis is generally utilized in the treatment of natural materials.

Pyrolysis is a thermochemical treatment, which can be applied to any natural item. In this treatment, material is presented to high temperature without oxygen.Because of that, material goes through physical and chemical partition into various particles. Pyrolysis of natural substances produces volatile materials and leaves a solid material that mainly consists of carbon. Outrageous pyrolysis which leaves carbon as a buildup is called carbonization. Pyrolysis is considered as the first step in processes of gasification or ignition. It is the process of material degradation that is unique in relation to different cycles like ignition and hydrolysis as it doesn't include the addition of different reagents like oxygen in burning or water in hydrolysis. Pyrolysis produces solids, liquids and gases.[25]

1.9.1 General process of pyrolysis

Pyrolysis by and large consists of heating the material over its disintegration temperature, breaking the compound bond in a material. The parts typically become smaller however they may join to create residues with bigger molecular mass. The starting material is heated in a vacuum or in an inert environment in order to stay away from compound side reactions like ignition or hydrolysis. Pyrolysis in a vacuum also brings down the boiling point of the byproducts, that helps in improving their recovery.

At the point when material is heated at high temperatures, the accompaniying cycles happens in progressive stages.

- Under 100 ^{0}C, volatiles including water fumes vanish. Heat-sensitive nutrients such as vitamin C and proteins also disintegrate at this stage.
- At 100 ^{0}C or marginally higher, any water that is present in the material is likewise dissipated. Water that is present in crystal structure of hydrates also removes at higher temperature.
- Between 100 and 500 ^{0}C, numerous organic molecules breakdown. Gases and volatile compounds leave the material and some of them condense as smoke. This cycle additionally absorbs energy. The disintegration items ordinally contain water, carbon monoxide and carbon dioxide. The non-volatile materials contain huge amount of carbon.
- At 200-300 ^{0}C, if oxygen is available, the carbonaceous material begins to consume. When the ignition begins, the temperature rises immediately. At this stage, a portion of the nitrogen that is present in the residue is oxidized into nitrogen oxides. Sulphur and different components also oxidized and volatilized at this stage.
- Once burning of carbonaceous material is finished, only ash remains behind.[26]

1.9.2 Types of pyrolysis

Complete pyrolysis of natural matter leaves a solid residue that comprises generally of elemental carbon. This process is called carbonization. Other sort of pyrolysis includes:[29]

- Methane pyrolysis
- Dry distillation
- Destructive distillation

- Cracking
- Thermal depolymerization

1.9.3 Morphology change during pyrolysis

Chemical reaction and physical changes during the pyrolysis cycle can change the morphology of MOFs to carbon-based materials. Quite possibly the most widely recognized morphology changes in the carbonization is the development of nanotubes. The metal particles in MOFs is decreased to metal nanoparticles via carbon or different reductants in the pyrolysis interaction. With the presence of natural ligands or outer carbon sources, these metal nanoparticles can catalyze the development of carbon nanotubes.

For the simple development of carbon nanotubes from MOFs, a system is proposed. In this technique, MOFs were treated by low temperature pyrolysis under Ar insurance. Gases were delivered in this interaction to lessen metal particles to metal nanoparticles. The leftover natural moiety at that point went about as the structural unit of carbon nanotubes. Other than the development of CNTs, the other ordinarily utilized system is to exploit the delivered gas during pyrolysis to adjust the carbon morphology. In this strategy after pyrolysis, a lot of gas is released prompting the development of foam-like porous and permeable carbon networks.[27]

1.9.4 Carbonization

Carbonization is a pyrolytic reaction. It is an unpredictable cycle where numerous reactions happen simultaneously like dehydrogenation, condensation, hydrogen transfer and isomerization. Carbonization is exothermic reaction which implies that it is self-maintaining and can be utilized as a wellspring of energy that doesn't create carbon dioxide. Template carbonization is isolated into processes in order to control morphology and pore design of carbon materials. Carbon materials in lamellar, cylindrical and foam morphology are incorporated by utilizing inorganic layered compounds as template. Microporous carbons are set up by utilizing zeolites as format and mesoporous carbons by utilizing silicas and metal-organic structures. Carbonization is the cycle where material is treated at high temperatures to eliminate the noncarbon components as volatile gases like methane, hydrogen, nitrogen, water, carbon monoxide, carbon dioxide,ammonia and different gases. The removal of these

materials diminishes the mass of material from 55 to 60 wt.%. Carbonization and activation are the main cycles in the advancement of low-cost activated carbon.[28]

1.10 Literature Review

The hydrogen evolution reaction (HER) and oxygen evolution (OER) assumes a fundamental part in numerous energy storage and transformation processes, including water splitting and regenerative power devices. The noble metal catalysts consisting of Pt, Ir, and Au are the best electrocatalysts for the HER and OER however because of their significant expense, shortage and low security, endeavors are being made to supplant them. Subsequently, it is important to foster effective, low-cost, and harmless non-noble metal electrocatalysts.[29]

In such manner, metal-organic frameworks (MOFs) have been promising candidate for HER and OER. MOFs have different compositions, enormous surface area, tunable pore designs and they are effectively functionalized. MOFs based catalyst displays superb catalytic performance for HER and OER.[30]

As a class of metal-organic frameworks (MOFs), Zeolitic imidazolate structures (ZIFs) are progressively mainstream. ZIFs are made out of tetrahedrally organized transition metal ions (Fe, Co, Cu and Zn) associated by imidazolate linkers. ZIFs have amazing chemical and thermal stability due to their microporous construction and enormous surface areas and tunable pore opening.However, they have poor conductivity due to insulating behavior of organic ligands. There are various approaches to expand the effectiveness of these materials.[31]

One path is to prepare nanoparticles of materials and the alternate way is taking conductive help from introduction of graphene, graphene oxide, and carbon nanotubes. Graphene is another class of conductive material, have 2D aromatic monolayers of carbon atoms. Graphene is a material of interest because of its enormous surface area, good electrical conductivity and better stability.[32]

1.11 Characterization: principles and analysis

1.11.1 X-Ray diffraction (XRD)

XRD is a typical strategy used to check the purity and phase identification of the crystalline materials and gives information about atomic spacing and dimensions of the unit cell. This technique works on the principle of constructive interference which happens between monochromatic X-rays and the crystalline material. In the crystal lattice, X-rays disperse on hitting with the electrons of an atom. This scattering phenomenon is called elastic scattering. Waves produced in the result of this process is determined by the Bragg's law:

$$2d\sin\theta = n\lambda$$

Where d signifies lattice spacing, θ gives information about the incident angle, λ represents the wavelength of X-rays, and n is an integer.[33]

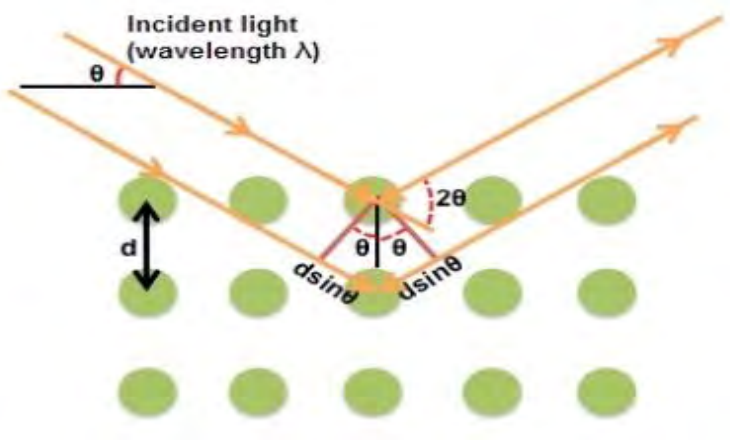

Figure 1.4 X-rays diffraction from atoms of crystal

1.11.2 Fourier transform Infrared Spectroscopy (FTIR)

FTIR spectroscopy is one of the most important analytical technique used to characterize natural, polymeric, and inorganic materials. This technique involves the intervention of infrared light with the sample. A broad band of near infrared (NIR) to far infrared (FIR) is required for FTIR analysis of the sample. All possible wavelengths are collected by FTIR. FTIR gives advantage over classical spectrophotometer having very short wavelength range, as the measuring range of FTIR is very high.

An FTIR instrument includes IR source, sample holder, detector and computer. Infrared radiations are emitted from the glowing black body and allowed to pass through the aperture where the controlled amount of energy is provided to the test sample. Specific frequencies that are characteristics of the molecular vibrations of the sample are absorbed and the rest are transmitted. The beam reaches to detector and recorded as interferogram. Lastly, the resultant signal is digitized, and computer Fourier transform function is applied on it.[34]

1.11.3 Thermogravimetric Analysis (TGA)

TGA is the technique that use the decomposition pattern of the sample for identification of the compounds. The purity of minerals, inorganic compounds, and organic materials can be determined by thermogravimetric analysis. This technique is used to study the thermal stability of the sample. TGA involves the study of changes in physiochemical properties of the materials by changing the temperature at fixed rate of heating. The specimen is subjected to a controlled temperature programmed, in an inert atmosphere. The sample is provided with heat at different time intervals up to desired range of temperature. With respect to time and heat the instrument measures the weight loss of the sample. Thermal stability for a given sample can be find out from the graph plotted between the temperature and weight loss.[35]

1.11.4 Scanning Electron Microscope (SEM)

The scanning electron microscope is commonly used to study the surface morphology of the materials. When sample is irradiated, electrons are emitted from it and gives the information about topography, composition, crystalline structure and morphology.

SEM is based on the principle that image is formed when electrons undergo interaction with atoms of sample. As a result of such interaction different signals are produced. By collecting such signals, an image is formed. The SEM analysis is performed under vacuum to avoid the interactions of electrons with free gas molecules.[36]

SEM instrument consist of following main components:

- Electron gun
- Column (condenser lens, objective lens and detector)
- Vacuum

1.11.5 Energy Dispersive X-RAY Spectroscopy (EDX)

Energy-dispersive X-ray spectroscopy (EDX) is an analytical strategy utilized for the elemental and chemical examination of the sample. In EDX, every element has a unique atomic structure and design permitting the remarkable arrangement of peaks on its electromagnetic emission spectrum. The peak positions are anticipated by the Moseley's law. In this technique a light emission is engaged into the sample. Electrons in the ground state are energized in an internal shell while making an electron hole. An electron from the external shell fills this opening and the distinction in energy between the higher and lower energy shell is delivered as X-ray which is specific for that material.[37]

1.12 Aims and Objectives

The aim of this research work is to synthesize ZIF-67 and ZIF-8 and their composites with GO as an electrode material. Simple mixing method (stirring and sonication) was used for synthesis followed by their characterization through different techniques. Electrochemical properties were studied by using LSV, EIS and Tafel slope.

1.12 Plan of work

The plan of work includes:

(1) Synthesis of ZIF-67, ZIF-8 and their carbonization
(2) Synthesis of GO, ZIF-67/GO, ZIF-8/GO and their carbonization
(3) Structural characterizations are performed by using XRD, FTIR, TGA, BET, SEM and EDX
(4) Electrochemical studies were done by using Linear sweep voltammetry (LSV), Electrochemical impedence spectroscopy (EIS) and Tafel slope

CHAPTER 2

Experimental

This chapter will give details of chemicals used in the synthesis of ZIF-67 and ZIF-8 and its composites. It will likewise include synthesis protocols, methods and an introduction of characterization techniques utilized. Finally, there will be an outline of electrochemical procedures used to check the activity of catalysts for HER and OER.

2.1 Synthetic protocols: reaction type, purification, and analysis

Nanomaterials have a wide scope of uses and their performance relies strongly on their shape and size. In this manner, an exertion has been made. Because of enormous number of uses of ZIF-67 and ZIF-8, the preparation of these nanomaterials in controlled way has acquired a lot of significance. Up until now, ZIF-67 and ZIF-8 in different nanostructures like hollow spheres, nanowires and nanotubes have been integrated, however everyone of these courses have a few difficulties. One of these difficulties is the ability of these nanoparticles to develop into an enormous and irregular particle. The subsequent challenge faced by the scientists is the phase purity of the end product.

In this way, to defeat these difficulties, there is a need to foster a more reliable and simple preparation method to get pure nanomaterials. In the present work, simple mixing method (stirring and sonication) was applied. This strategy is simple, easy and did not require any catalyst or costly harmful material. So, it is the best technique for the low-cost synthesis of nanomaterials.

2.2 Chemicals and reagents

For the synthesis of materials, utilization of good quality synthetic substances and solvents was guaranteed to get purity in the final product. Cobalt nitrate, zinc nitrate, 2-methyl imidazole, potassium permanganate and sodium nitrate were bought from Sigma Aldrich (Germany) and were utilized without any further purification. Deionized water utilized in the readiness of electrolyte was taken from the deionizer set in the

laboratory. KOH pellets for the readiness of electrolyte is likewise taken from Sigma Aldrich, Germany. Nafion solution is bought from Merck. Sulphuric acid was 99% pure and secured from BDH. The solvent utilized in the synthesis of nanoparticles was methanol which was purchased from Sigma Aldrich.

2.3 Drying of solvents

The solvents used in the synthesis process were ethanol, methanol and deionized water. To eliminate any dampness or impurity from solvents, they were dried before use as follows:

2.3.1 Drying of ethanol and methanol

Ethanol and methanol were first distilled and refined and then further purified by drying under reflux by standard method with Mg turnings as a drying agent. Iodine crystals were utilized as indicator.

2.4 Instrumentation

2.4.1 X-ray diffraction analysis (XRD)

Ni-filtered Cu Kα radiations were used to record X-ray diffraction patterns in transmission mode. The samples were kept 0.02 at diffraction angle 2θ = 5-60^0 with the help of X-ray diffractometer model Xpert Pro by PANalytical Holland.

2.4.2 FT-IR spectroscopic studies

FTIR-ATR Spectrophotometer of model 1000 Perkin Elmer were used to identify different functional group. Frequency range was kept from 450-4500 cm^{-1} throughout the analysis.

2.4.3 Thermogravimetric Analysis

The thermal stability of material is elucidated by Perkin Elmer. The temperature range was kept from 25-600 ^{0}C at heating rate of 20 ^{0}C /min and analysis was performed under nitrogen atmosphere.

2.4.4 Scanning Electron microscope

SEM images were collected using VEGA3 TESCAN field emission scanning electron microscope. Different resolutions were applied to take images from 200 µm to 10 µm using an accelerating voltage of 20 kV.

2.5 Purification of graphene powder

1 g of graphene powder is purified by adding 10 mL of nitric and 10 mL of sulphuric acid. The solution was stirred for 3 hours and left for 4 days to settle down. The subsequent item was washed 3-4 times with HCl to eliminate all impurities.

2.6 Synthesis of graphene oxide (GO)

Graphene oxide was integrated utilizing Hummers method. GO is prepared by stirring 1 g of graphene and 0.6 g of sodium nitrate into 23 mL of sulphuric acid in an ice bath. To this solution add 4 g of potassium permanganate. It was added gradually so that temperature does not exceed from 20 ^{0}C. Removed the ice bath and solution was leaved at 35 ^{0}C for 30 mins. After 20-30 mins the mixture becomes pasty which was brownish grey in color. To this solution 50 mL of water is added causing an increase in temperature to 100 ^{0}C. The suspension was further diluted by adding 150 mL of warm water. This solution was treated with 3% hydrogen peroxide. As a result of addition of hydrogen peroxide , the suspension was turned bright yellow. The suspension was then filtered and washed three times with water. The obtained graphene oxide was dried at 60 ^{0}C.[38]

2.7 Synthesis of ZIF-67 and its Carbonization

To prepare ZIF-67, 2.32 g of cobalt nitrate hexahydrate was dissolved in 40 mL of methanol. Similarly, 2.463 g of 2-methyl imidazole was also dissolved in 40 mL of methanol. The above two solutions were mixed together. On the addition of 2-methyl imidazole in cobalt nitrate, the solution become purple in color which goes through sonication for 2 hours to accomplish uniform composition. The solution was leaved for 24 hours. Then the obtained product was isolated by centrifugation and washed with methanol several times, then dried at 60 ^{0}C overnight. In this way, ZIF-67 crystals are

obtained that are further carbonized in tube furnace at 700 ^{0}C for 2 hours at heating rate of 10 ^{0}C/min in an inert (Ar/N_2) atmosphere.[39]

2.8 Synthesis of composite of ZIF-67/GO

To prepare composite of ZIF-67 with GO, 0.18 g of ZIF-67 was dispersed in 40 mL of methanol. In like manner, 0.018 g of GO was dispersed in 40 mL of methanol, then the above two solutions sonicated for 2 hours to achieve the maximum dispersion of ZIF-67 and GO in methanol. After sonication, solutions were mixed together. The resultant solution was continuously stirred for 1 hour. The obtained product was separated by centrifugation and dried at 60 ^{0}C overnight.[40]

2.9 Synthesis of Carbonized ZIF-67/rGO

In order to prepare carbonized ZIF-67/rGO, first composite of ZIF-67 with GO was prepared. 0.18 g and 0.018 g of ZIF-67 and GO was dispersed in methanol. The above two solutions were sonicated for 2 hours followed by stirring for 1 hour in order to achieve uniform composition. The obtained product was isolated by centrifugation and dried at 60 ^{0}C overnight. As a result of that ZIF-67/GO was obtained. The product then carbonized in tube furnace at 700 ^{0}C for 2 hours at heating rate of 10 ^{0}C/min in an inert (Ar/N_2) atmosphere.[41] The synthetic scheme is shown in **fig.2.1.**

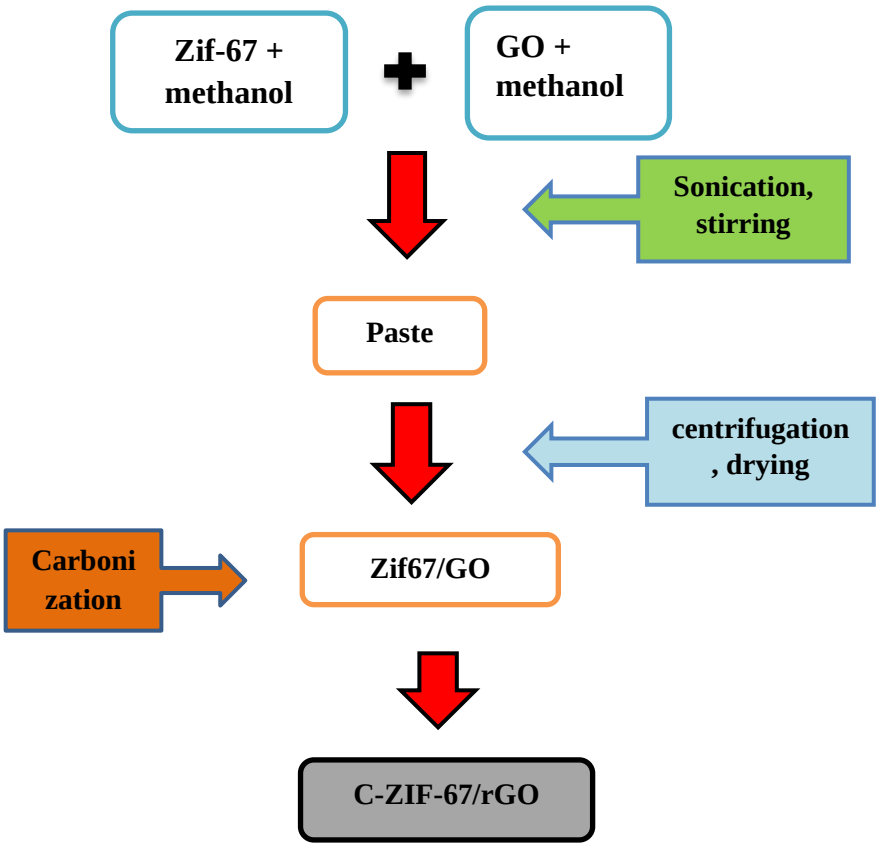

Figure 2.1 : Synthesis of C-ZIF-67/rGO

2.10 Synthesis of ZIF-8 and its Carbonization

To prepare ZIF-8, 2.38 g of zinc nitrate hexahydrate is dissolved in 40 mL of methanol. Similarly, 2.463 g of 2-methyl imidazole was also dissolved in 40 mL of methanol. The above two solutions were mixed together and constantly stirred for 2 hours. The solution was leaved for 24 hours without any disturbance. The obtained product was separated by centrifugation and washed with methanol several times, then dried at 60 ^{0}C overnight. In this way ZIF-8 crystals are obtained that are further carbonized in tube furnace at 700 ^{0}C for 2 hours at heating rate of 10 ^{0}C/min in an inert (Ar/N_2) atmosphere.[42]

2.11 Synthesis of composite of ZIF-8/GO

To prepare composite of ZIF-8 with GO, 0.18 g of ZIF-8 was dispersed in 40 mL of methanol. Likewise, 0.018 g of GO was also dispersed in 40 mL of methanol. The above two solutions sonicated for 2 hours to achieve uniform dispersion of ZIF-8 and GO in methanol. After sonication, solutions were mixed together and continuously stirred for 2 hours. The obtained product was separated by centrifugation and dried at 60 ^{0}C overnight.[43]

2.12 Synthesis of Carbonized ZIF8/rGO

In order to prepare carbonized ZIF-8/rGO, first composite of ZIF-8 with GO was prepared. ZIF-8 and GO were dispersed in methanol. The above two solutions goes through sonication for 2 hours followed by stirring for 1 hour. The obtained product was separated by centrifugation and dried at 60 ^{0}C overnight. ZIF-8/GO then carbonized in tube furnace at 700 ^{0}C at heating rate 10 ^{0}C/min in an inert (Ar/N_2) atmosphere.[44] The procedure for the synthesis of carbonized ZIF-8/rGO is shown in **fig.2.2.**

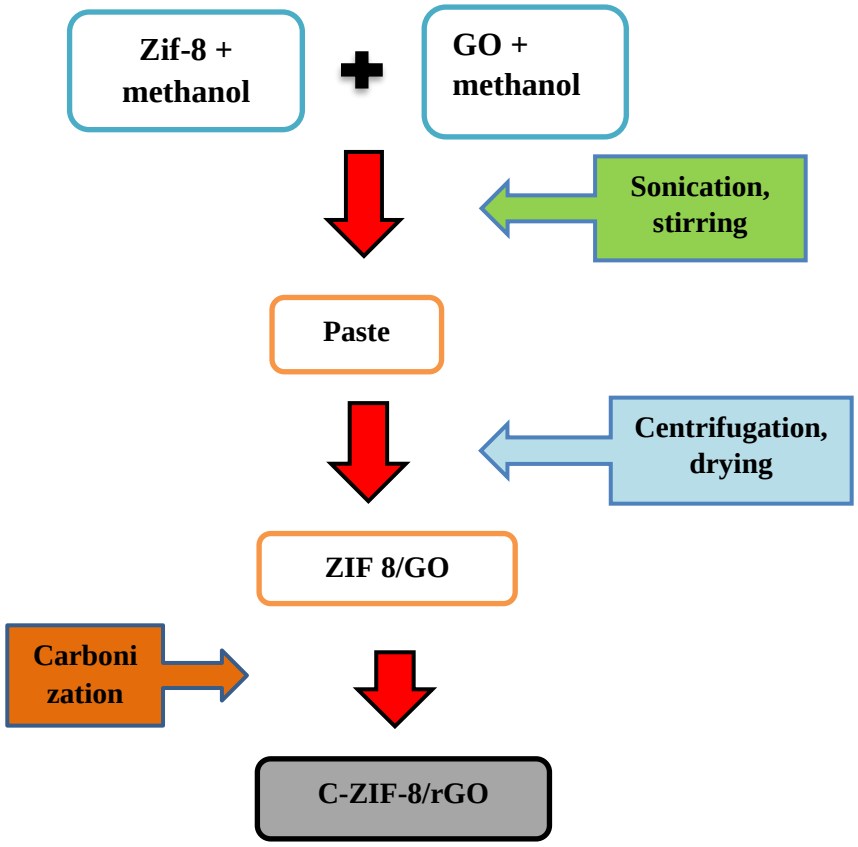

Figure 2.2 Synthesis of C-ZIF-8/rGO

2.13 Electrochemical measurements

For electrochemical measurements, a three electrode system was used. One was glassy carbon (working electrode), second Pt wire (counter electrode) and third Ag/AgCl (reference electrode). All measurements were carried out using 1M KOH solution for OER and 0.5M H_2SO_4 solution for HER.

2.13.1 Ink and electrode preparation

To prepare ink for working electrode, 3 mg of catalyst was dissolved in 800 μL ethanol having 100 μL Nafion. Then the solution was sonicated for 2 hours. By using micropipette this ink was coated on working glassy carbon (GC) electrode which was dried before use and then used for measurements.

Chapter 3

Results and Discussion

In this chapter, details of results of characterization techniques will be given. In the end conclusions of the present research are also given. The synthesized nanoparticles of ZIF-67 and ZIF-8 and their composites with GO were subjected to different characterization techniques including XRD, IR, TGA and BET.

3.1 X-Ray diffraction studies (XRD)

The geometry and crystallinity of the samples was characterized by XRD analysis. The PXRD analysis of ZIF-67 clearly confirms the crystallinity in the synthesized materials. **Fig.3.1** shows the XRD pattern of ZIF-67 where all the peak positions and the crystallinity of our synthesized material is clearly matching with the reported XRD pattern of ZIF-67. The diffraction peaks appear at 2θ values of 7.4°, 10.61°, 12.84°, 14.7°, 16.4°, and 18.31° which corresponds to the crystal planes (011), (002), (112), (022), (013) and (222).[45]

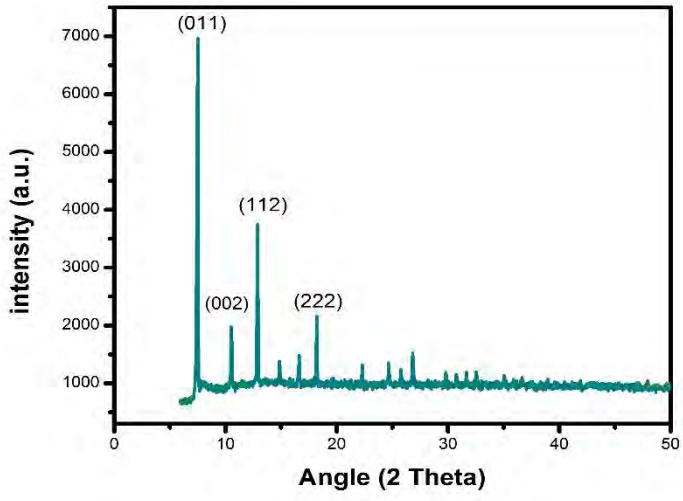

Figure.3.1 X-ray diffractogram of ZIF-67

The simulated pattern of ZIF-67 is shown in **fig.3.2.**[46]

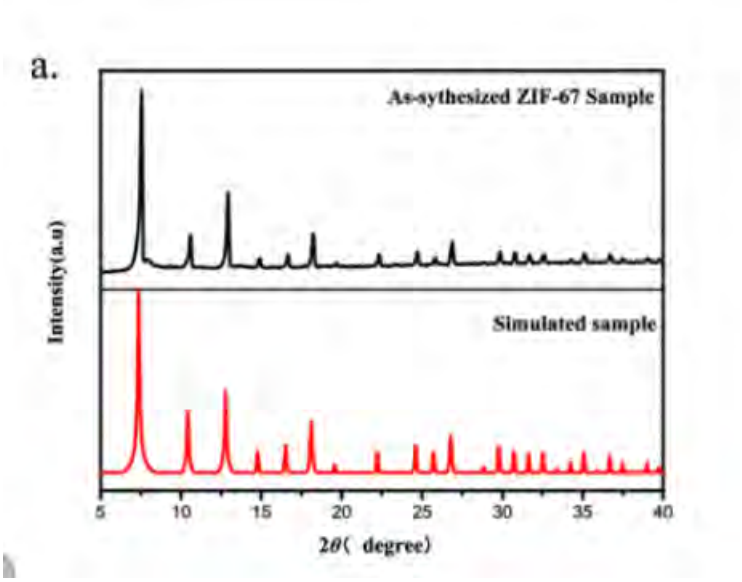

Figure 3.2 Simulated pattern of ZIF-67

ZIF-8 has a cubic structure with tetrahedral geometry that has been confirmed by XRD results shown in **fig.3.3.** In diffractogram of ZIF-8, all diffraction peaks appear at 2θ values of 7.35^{o}, 10.35^{o} , 12.83^{o} , 14.65^{o} , 16.4^{o} , and 18.05^{0} corresponding to the crystal planes of (011), (002), (112), (022), (013) and (222). These peaks confirm the synthesis of ZIF-8.[46]

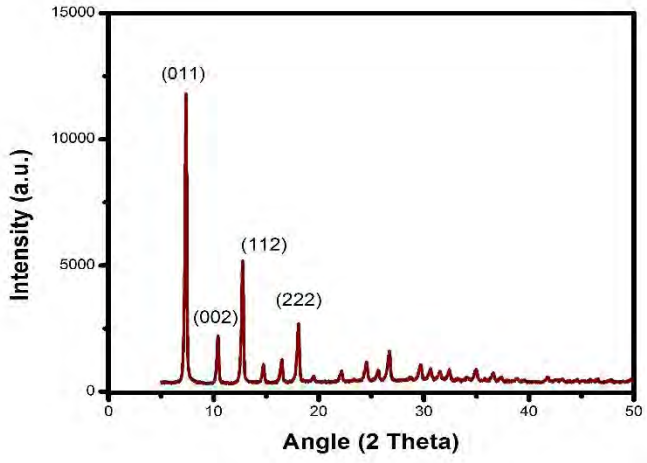

Figure.3.3 X-Ray diffractogram of ZIF-8

The simulated pattern of ZIF-8 is given in **fig.3.4.**[48]

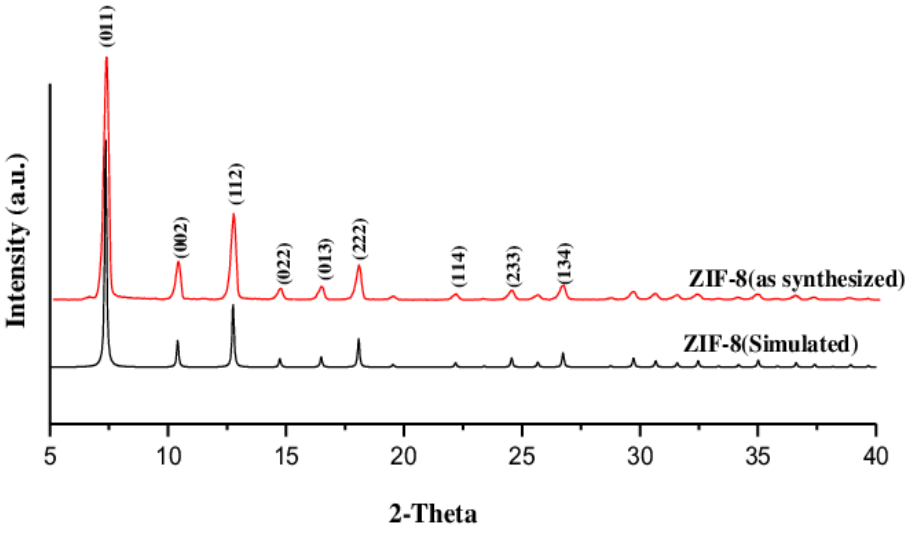

Figure.3.4 Simulated pattern of ZIF-8

The X-Ray diffractogram of GO is depicted in **fig.3.5.** In diffractogram of GO, the peak observed at 10.78° is assigned to (002) crystal plane of GO. This peak is due to an interlayer spacing present between sheets of graphene oxide. The peak at 42.72° (001) is due to incomplete oxidation of graphite powder.[47]

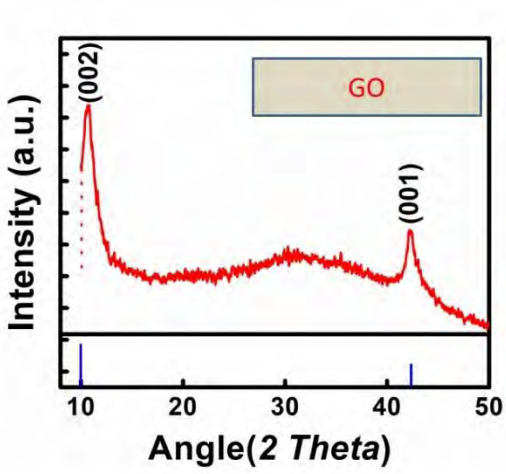

Figure.3.5 X-Ray diffractogram of GO

The X-Ray diffractogram of composite of ZIF-8 with GO is shown in **fig.3.6.** The peak at 10.78° is attributed to (002) plane of GO while the diffraction peaks at 12.83°, 14.7°, 16.4° and 18.05° corresponds to the (112), (013), (222) and (022) crystal planes of

ZIF-8. The decrease in the intensity of peak at 42.72° indicates the almost complete oxidation of graphite.[48]

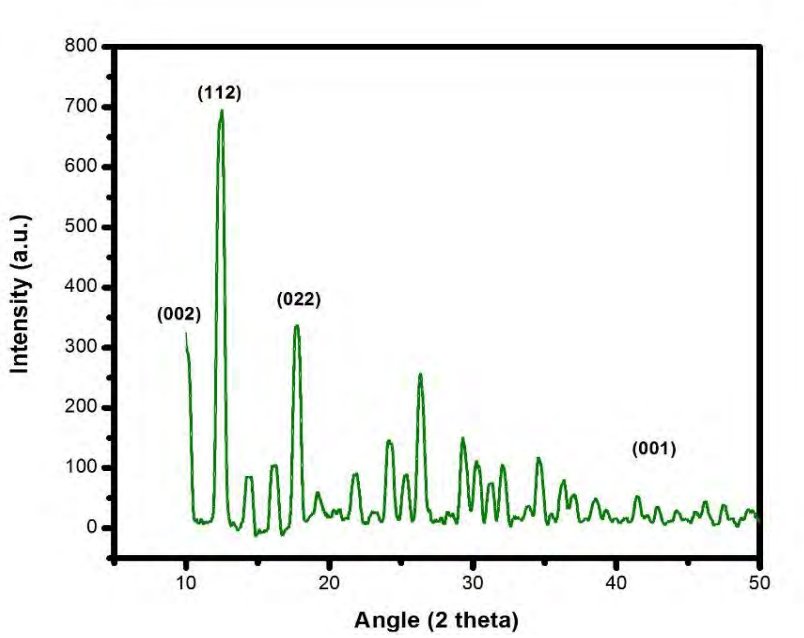

Figure.3.6 X-Ray diffractogram of ZIF-8/GO

3.2 Infrared Spectroscopy (FTIR)

The IR spectrum of synthesized GO is shown in **fig.3.7.** IR provides the information for the presence of different functional groups in GO. The peaks at 1032 cm^{-1} and 1350 cm^{-1} are due to CO and C-OH bond. The peak at 1600 cm^{-1} is attributed to C=C. The peak at 1700 cm^{-1} corresponds to stretching vibration of C=O. A broad peak in the region around 3000-3400 cm^{-1} is due to stretching vibration of a hydroxyl group [49]

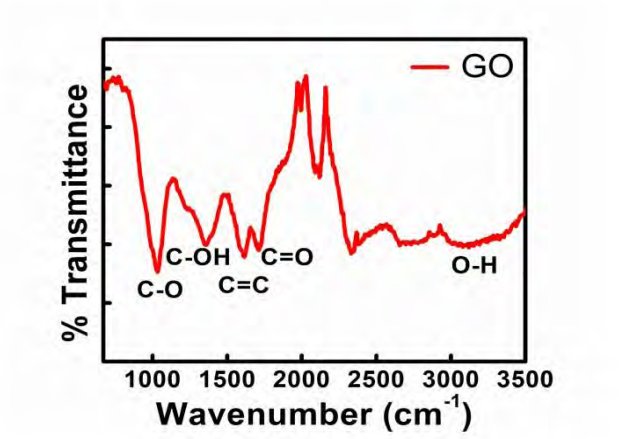

Figure 3.7 FTIR spectrum of GO

IR spectrum of ZIF-67 is shown in **fig.3.8.** Peaks like 763, 993,1147 and 1179 are due to out of plane and in plane stretching and bending of 2-methyl imidazole group. The peak at 576 cm^{-1} corresponds to Co-N bond. C-N bond shows its peak at 1300 cm^{-1}. The peaks at 1409 cm^{-1} and 1580 cm^{-1} are attributed to stretching mode of C=N bond. The peaks obtained at 2929 and 3139 cm^{-1} were due to stretching of C-H from aliphatic methyl group and aromatic ring of 2-MIM.[50]

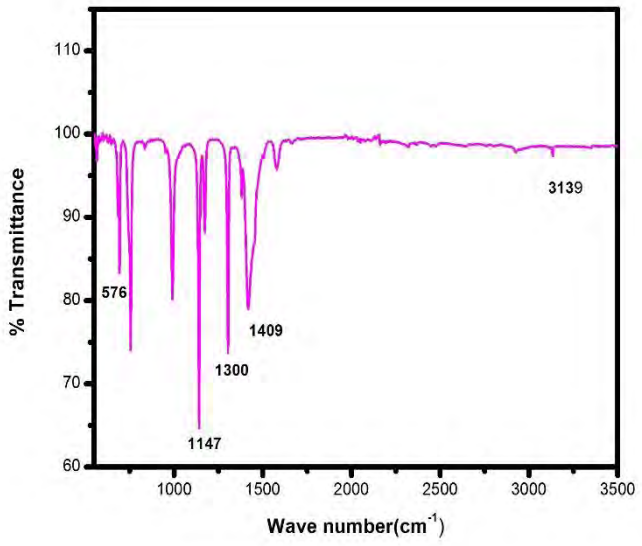

Figure.3.8 FTIR spectrum of ZIF-67

FTIR spectrum of composite of ZIF-67 with GO is shown in **fig.3.9.** In this spectrum, the peaks at 749 cm^{-1}, 997 cm^{-1},1188 cm^{-1} are attributed to out of plane bending of 2-MIM in ZIF-67. The peak at 1305 cm^{-1} is due to C-N bond. Absorption peaks related to C=O, C=C, and hydroxyl group disappeared. Certain GO peaks like 1052 cm^{-1} and 1382 cm^{-1} corresponding to C-O-C and C-OH also appeared in spectra that confirmed the formation of composite of ZIF-67 with GO.[51]

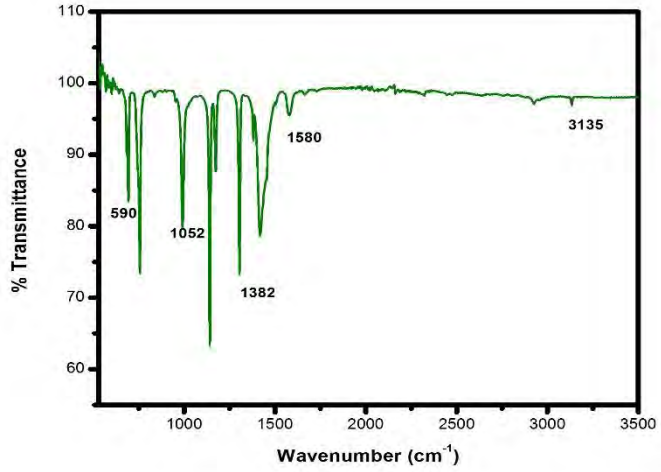

Figure.3.9. FTIR spectrum of ZIF-67/GO

Fig.3.8 shows the FTIR spectrum of Carbonized ZIF-67/rGO. Peaks in the range of 600-1580 cm^{-1} completely disappear because the imidazole rings are collapsed during the calcination process. No sharp peaks related to oxygen functional groups appeared that confirm effective reduction of GO into rGO. Extending vibration around 1600 cm^{-1} were due to development of sp2 carbon structure of rGO. OH group stretching vibration at 3400 cm-1 was absent because of deoxygenation.[52]

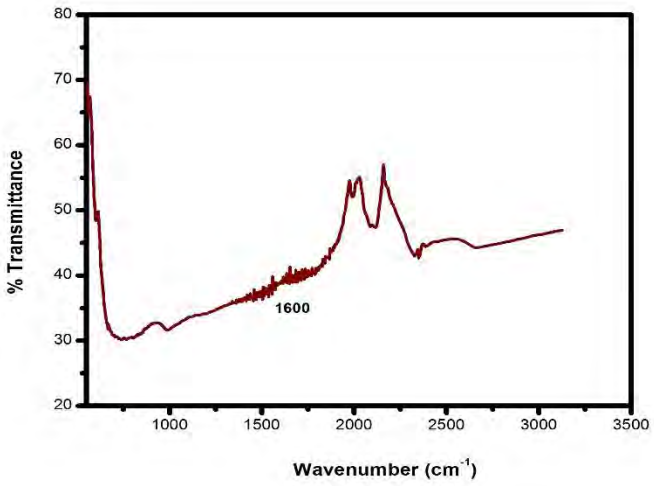

Figure 3.10 FTIR spectrum of C-ZIF67/rGO

Fig.3.10 represents the IR spectrum of ZIF-8. ZIF-8 also has a cubic structure with tetrahedral geometry that has been confirmed by XRD result. The peak at 590 cm^{-1} is attributed to Zn-N bond. Out of plane stretching and bending of 2-methyl imidazole group is shown by peaks like 761 cm^{-1}, 988 cm^{-1}, 1137 cm^{-1}, and 1184 cm^{-1}. C-N shows its peak at 1305 cm^{-1}. The peaks at 1420 and 1581 are due to in plane bending of C=N bond. The peaks obtained at 2927 and 3123 were attributed to stretching of C-H from aliphatic methyl group and aromatic ring of 2-MIM.[53]

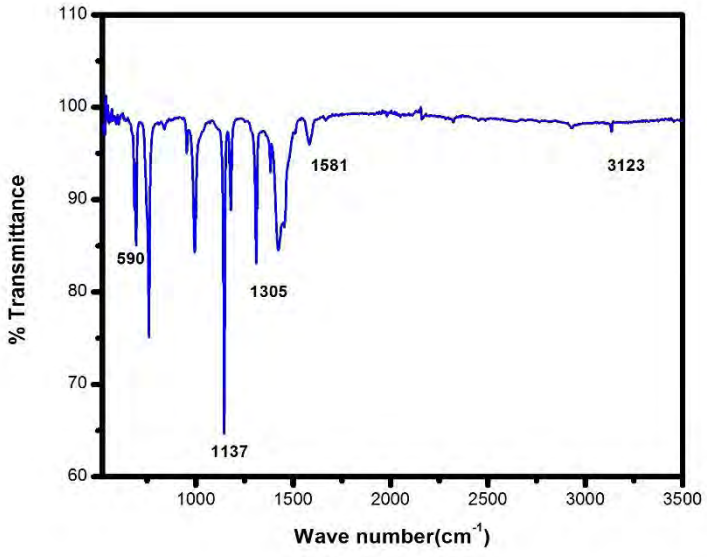

Figure.3.11. FTIR spectrum of ZIF-8

FTIR spectrum of composite of ZIF-8 with GO is given in **fig.3.11.** In this spectrum, Zn-N peak appeared at 590 cm^{-1}. The peaks at 749 cm^{-1}, 997 cm^{-1}, and 1188 cm^{-1} are attributed to out of plane bending of 2-MIM in ZIF-8. The peak at 1305 cm^{-1} corresponds to C-N bond. Absorption peaks related to C=C, C=O and hydroxyl group of GO disappeared. Certain GO peaks like 1054 cm^{-1} and 1382 cm^{-1} also appeared in spectra that confirmed the formation of composite of ZIF-8 with GO.[54]

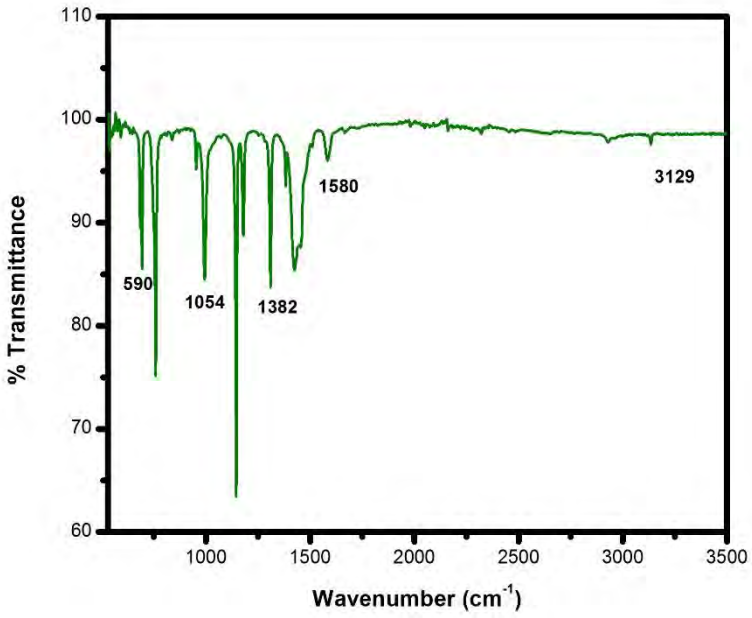

Figure.3.12 FTIR spectrum of ZIF-8/GO

Fig.3.12. shows the FTIR spectrum of carbonized ZIF-8/rGO. After heat treatment, there was no characteristic peak for ZIF-8 due to effective and complete conversion of ZIF-8/GO into carbon. Peaks in the range of 600-1580 cm^{-1} completely disappeared because the imidazole rings are entirely removed during the calcination process. No sharp peaks related to oxygen functional groups appeared due to reduction of of GO into rGO. Stretching vibration around 1600 cm^{-1} were due to development of sp^2 carbon structure of rGO.[55]

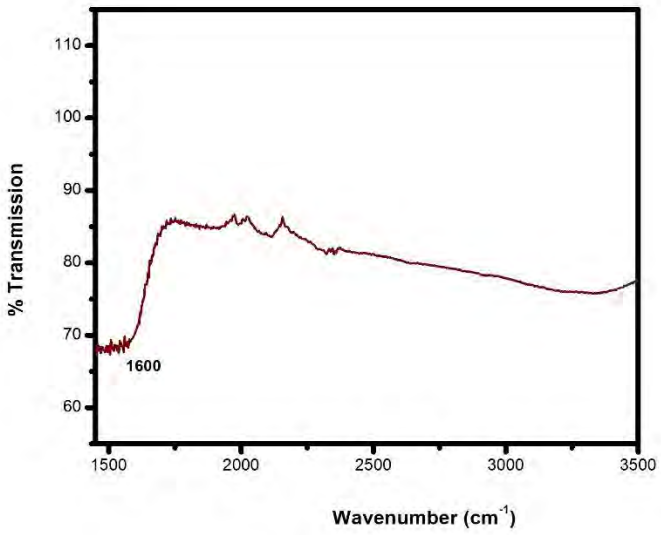

Figure.3.13. FTIR spectrum of C-ZIF-8/GO

3.3 Thermogravimetric analysis

The thermal stability of ZIF-67 was checked by thermogravimetric analysis. The sample was subjected to thermal treatment starting starting from room temperature to 600 ^{0}C. **Fig.3.14** represents the TGA curve of ZIF-67, where two major weight losses were observed, attributed to the decomposition of ZIF framework and solvent molecules. The weight loss that was observed after 400 ^{0}C corresponds to the decomposition of framework of ZIF-67. The weight loss that was observed below 250 ^{0}C is due to removal of unreacted species and solvent molecules.[56]

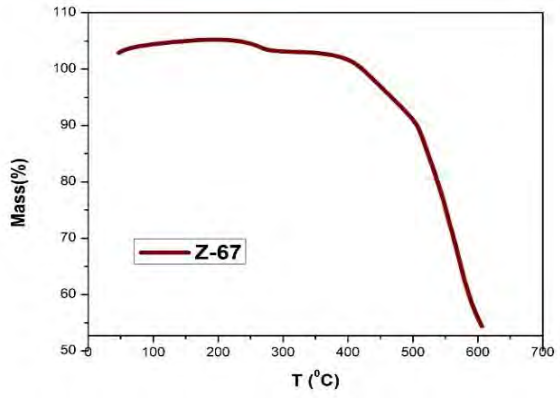

Figure.3.14 TGA curve of ZIF-67

3.4 BET results

The specific surface area, pore size and pore volume were derermined by N_2 adsorption-desorption isotherms. The samples that were characterized indicated that all nanocomposites possessed microporous structures. The BET results show that, in comparison with ZIF-67, ZIF-67/GO has increased surface area. Similarly, ZIF-8/GO has more surface area than ZIF-8. Similarly, the pore volumes measured for ZIF-67/GO and ZIF-8/GO is larger than the ZIF-67 and ZIF-8. Thus it is concluded that the introduction of GO caused an increase in surface area and total pore volume of the material. Table 3.1 shows the pore structure parameters like surface area (m^2/g), pore volume (cm^{-3}/g), and pore size (nm).

Table 3.1. Pore structure parameters

Material	**BET surface area (m^2/g)**	**Pore volume (cm^{-3}/g)**	**Pore size (nm)**
ZIF-67	**202**	**0.756**	**1.847**
ZIF-67/GO	**1222.31**	**1.125**	**3.169**
ZIF-8	**71.33**	**0.124**	**2.211**
ZIF-8/GO	**1114**	**0.643**	**2.897**

SEM, EDX and TGA results are awaiting.

3.5 Electrochemical studies of ZIF-67 for both HER and OER

For **HER** and **OER**, electrochemical properties was studied using linear sweep voltammetry (LSV), electrochemical impedence spectroscopy (EIS) and tafel slope.

3.5.1. Linear sweep voltammetry (LSV)

LSV curves were recorded at scan rate of 50mV/sec. The potential range was kept between (+0.2)-(-1.0) Vs. RHE using 0.5 M H_2SO_4 solution for HER and (+1)-(+2) Vs. RHE using 1M KOH for OER in three electrode system. Pt and Ag/AgCl electrodes were used as counter and reference electrode. **Fig.3.15.** shows the linear sweep voltammograms of ZIF-67, ZIF-67/GO, carbonized ZIF-67 and carbonized ZIF-67/rGO for HER.

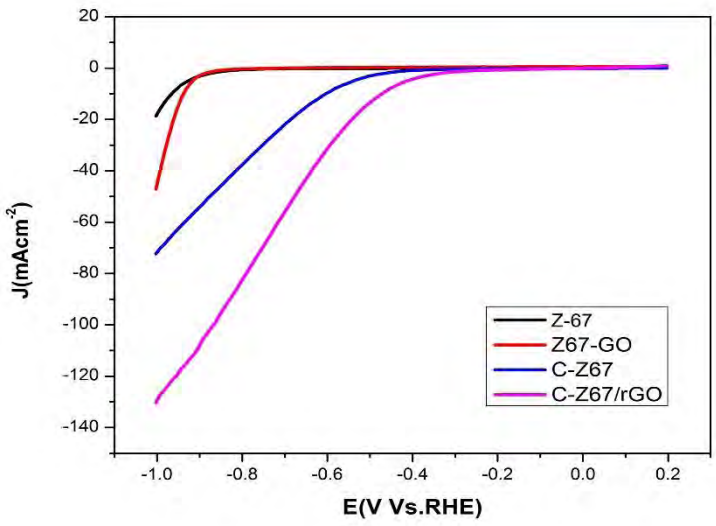

Figure.3.15 LSV of ZIF-67 and its composite with GO for HER

These lsv curves show that C-ZIF67/rGO exhibits maximum current density of 130mA/cm^2 at onset potential of -0.30 mV among the four materials. Thermodynamic potential for HER through 2e$^-$ is 0V. Table 3.1 shows all results of LSV for ZIF-67 and its composites.

Table 3.2. Parameters calculated from LSV for HER of ZIF-67

Material	Onset potential (V)	Overpotential (E_{10})
ZIF-67	**-0.84**	**0.84**
ZIF-67/GO	**-0.82**	**0.82**
C-ZIF-67	**-0.40**	**0.40**
C-ZIF-67/rGO	**-0.30**	**0.30**

Fig.3.16. shows the linear sweep voltammograms of ZIF-67, ZIF-67/GO, carbonized ZIF-67 and carbonized ZIF-67/rGO for OER.

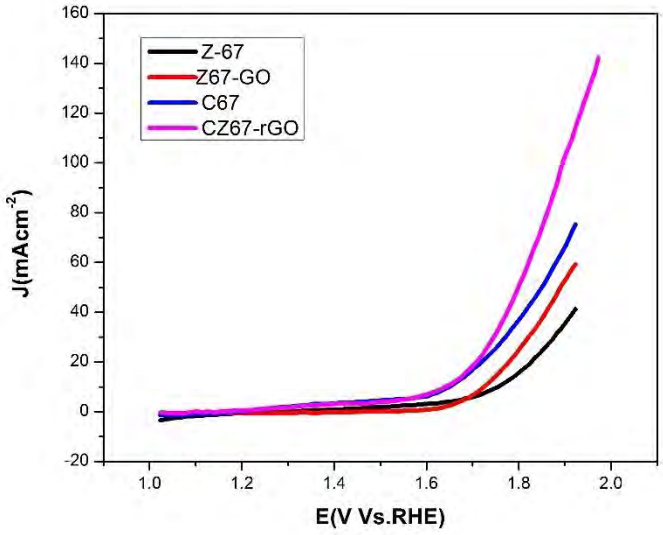

Figure.3.16 LSV of ZIF-67 and its composite with GO for OER

Here C-ZIF-67/rGO shows the maximun current density of 140mAcm^{-2} at the onset potential of 1.58 mV among the four materials. Thermodynamic potential for OER is 1.23 V. Table 3.2 shows all results of LSV for ZIF-67 and its composites.

Table 3.3. Parameters calculated from LSV for OER of ZIF-67

Material	Onset potential (V)	Overpotential (E_{10})
ZIF-67	**1.73**	**0.5**
ZIF-67/GO	**1.68**	**0.45**
C-ZIF-67	**1.62**	**0.39**
C-ZIF-67/rGO	**1.58**	**0.35**

3.5.2 Electrochemical Impedence spectroscopy (EIS)

EIS technique further confirms the catalytic activity of materials for HER and OER. This plot is recorded between real frequency on X-axis and imaginary frequency on Y-axis and frequency range is 1 Hz – 100 KHz respectively. EIS plots give the charge transfer resistance (R_{CT}). Smaller the diameter of the semicircle, smaller will be the charge transfer resistance and higher will be the conductivity of the material. **Fig.3.17.** and **Fig.3.18.** represents the EIS (Nyquist plot) of ZIF-67, ZIF-67/GO, carbonized ZIF-67 and carbonized ZIF-67/rGO for HER and OER.

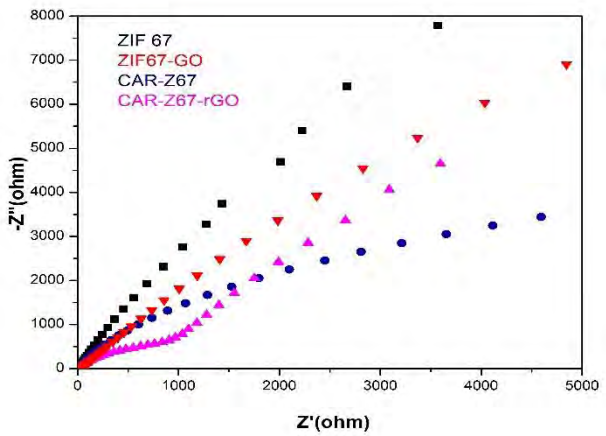

Figure 3.17 EIS (Nyquist plot) of ZIF-67 and its composite with GO for HER

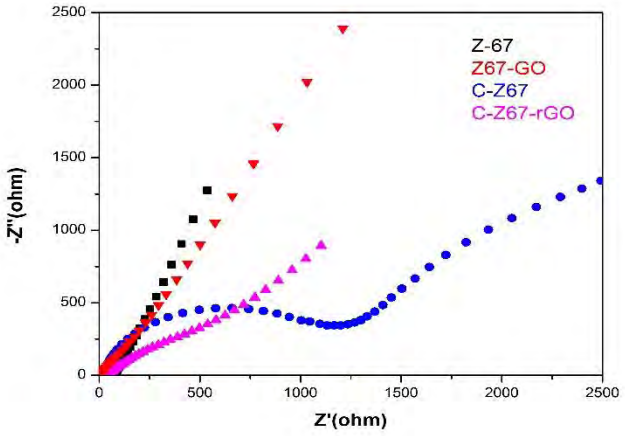

Figure.3.18 EIS (Nyquist plot) of ZIF-67 and its composite with GO for OER

Both these graphs clearly showed that C-ZIF-67/rGO has small semicircle among four materials which means that it has smaller charge transfer resistance and hence shows better conductivity.

3.5.3 Tafel slope

Tafel slope gives the information about how much overpotential has to be increased for an increase in reaction rate by factor ten. It is a curve between current on X-axis and overpotential on Y-axis respectively. Lower the tafel slope, better will be the catalyst for electrochemical activity. **Fig.3.19.** and **fig.3.20.** represents the tafel slope of ZIF-67, ZIF-67/GO, carbonized ZIF-67 and carbonized ZIF-67/rGO.

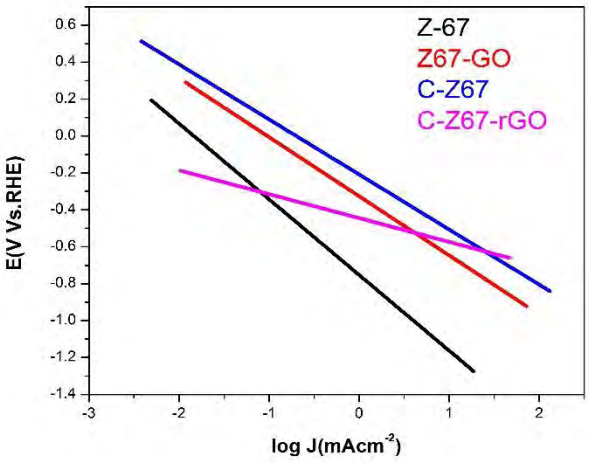

Figure. 3.19 Tafel plot of ZIF-67 for HER

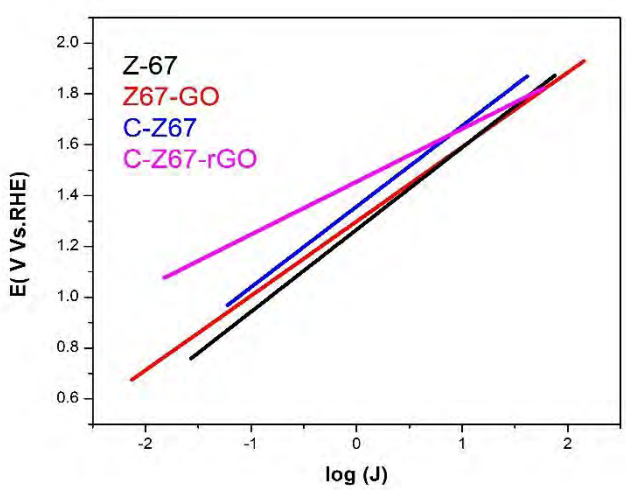

Figure. 3.20 Tafel plot of ZIF-67 for OER

Both tafel plots showed that among four materials, composite of carbonized ZIF-67 with rGO shows the least tafel slope of -58 $mVdec^{-1}$ for HER and tafel slope of -89 $mVdec^{-1}$ for OER.

Table.3.4 Tafel slope results of ZIF-67 for HER

Material	**Tafel slope ($mVdec^{-1}$)**
ZIF-67	**-129**
ZIF-67/GO	**-116**
C-ZIF-67	**-92**
C-ZIF-67/rGO	**-58**

Table.3.5 Tafel slope results of ZIF-67 for OER

Material	Tafel slope($mVdec^{-1}$)
ZIF-67	-136
ZIF-67/GO	-122
C-ZIF-67	-106
C-ZIF-67/rGO	-89

3.6 Electrochemical studies of ZIF-8 for HER and OER

Electrochemical studies were also done for ZIF-8 and its composites using linear sweep voltammetry (LSV), electrochemical impedence spectroscopy (EIS) and tafel slope.

3.6.1. Linear sweep voltammetry (LSV)

LSV curves were recorded at scan rate of 50mV/sec. The potential range was kept between (-0.2)-(-1.4) Vs. RHE using 0.5 M H_2SO_4 solution for HER and (0)-(+1.8) Vs. RHE using 1 M KOH for OER in three electrode system. Pt was used as counter electrode and Ag/AgCl was used as reference electrode. **Fig.3.21.** shows the LSV curves of ZIF-8, ZIF-8/GO, carbonized ZIF-8 and carbonized ZIF-8/rGO for HER.

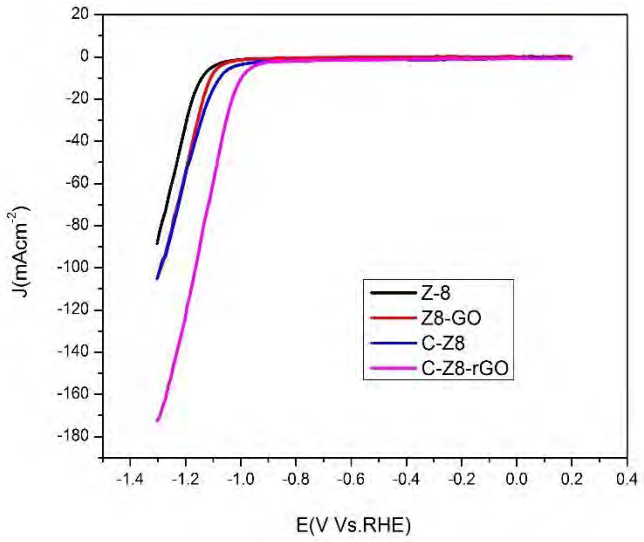

Figure.3.21 LSV curves of ZIF-8 and its composite with GO for HER

These LSV curves show that C-ZIF-8/rGO shows the maximum current density of 170mA/cm^{-2} at onset potential of -0.86 mV among the four materials. Table 3.5 shows all results of LSV for HER.

Table 3.6. Parameters calculated from LSV for HER of ZIF-8

Material	Onset potential (V)	Overpotential (E_{10})
ZIF-8	**-1.13**	**1.13**
ZIF-8/GO	**-1.10**	**1.10**
C-ZIF-8	**-0.92**	**0.92**
C-ZIF-8/rGO	**-0.86**	**0.86**

Fig.3.22. shows the LSV curves of ZIF-8, ZIF-8/GO, carbonized ZIF-8 and carbonized ZIF-8/rGO for OER.

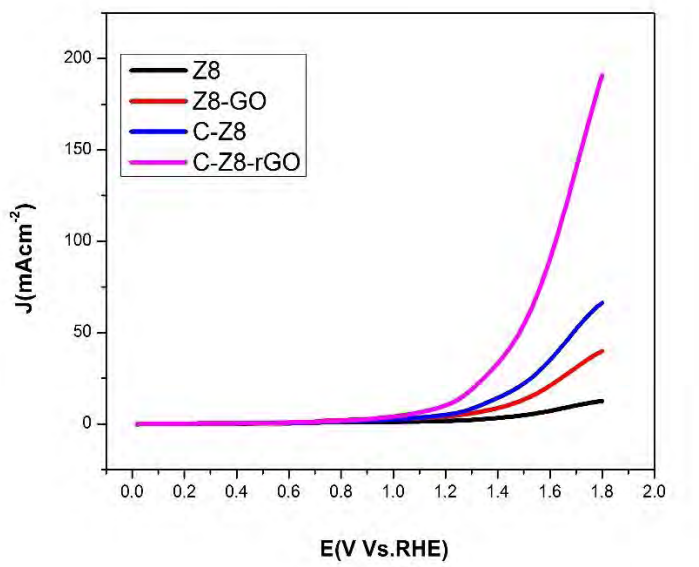

Figure.3.22 LSV curves of ZIF-8 and its composite with GO for OER

Here C-ZIF-67/rGO shows the maximum current density of 190mAcm^{-2} at the onset potential of 1.28 mV among the four materials and the thermodynamic potential for OER is 1.23 V. Table 3.6. shows all results of LSV for OER.

Table 3.7. Parameters calculated from LSV for OER of ZIF-8

Materials	**Onset potential (V)**	**Overpotential (E_{10})**
ZIF-8	**1.57**	**0.34**
ZIF-8/GO	**1.37**	**0.14**
C-ZIF-8	**1.33**	**0.1**
C-ZIF-8/rGO	**1.28**	**0.05**

3.5.2 Electrochemical impedence spectroscopy (EIS)

EIS technique assists the LSV in confirming the electrocatalytic activity of materials for HER and OER. This plot is recorded between real and imaginary frequency on X and Y-axis respectively. The frequency range is 1 Hz – 100 KHz. This technique gives information about charge transfer resistance. Larger the diameter of the circle, larger will be the charge transfer resistance and lower will be the conductivity of the material and vice versa. **Fig.3.23.** and **fig.3.24.** represents the EIS (Nyquist plot) of ZIF-8, ZIF-8/GO, carbonized ZIF-8 and carbonized ZIF-8/rGO for HER and OER.

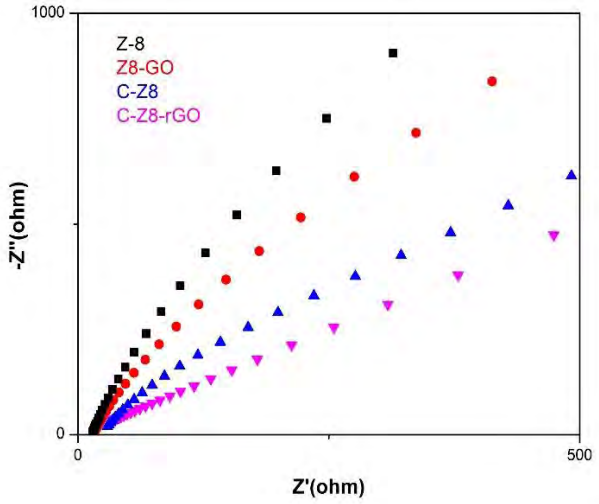

Figure.3.23 EIS (Nyquist plot) of ZIF-8 and its composite with GO for HER

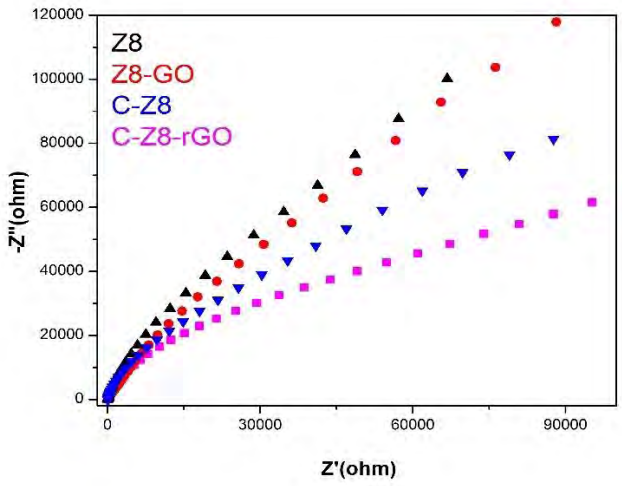

Figure.3.24 EIS (Nyquist plot) of ZIF-8 and its composite with GO for OER

Both these graphs showed that among the four materials, C-ZIF-8/rGO shows the smallest semicircle that indicates its lower charge transfer resistance which results into better catalytic activity.

3.5.3 Tafel slope

Tafel slope can be measured by taking log of current density on X-axis and overpotential on Y-axis respectively. It tells about how much overpotential has to be increased for an increase in reaction rate by factor ten. Lower the tafel slope, better will be the electrocatalytic activity of the material and vice versa. **Fig.3.25.** and **fig.3.26.** represents the tafel slope of ZIF-8, ZIF-8/GO, carbonized ZIF-8 and carbonized ZIF-8/rGO.

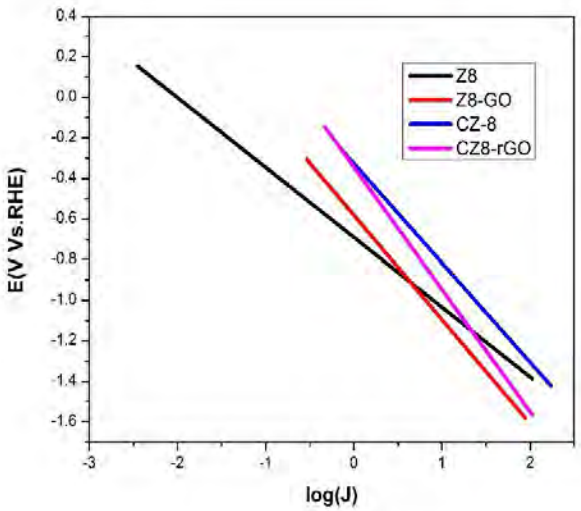

Figure. 3.25 Tafel slope of ZIF-8 for HER

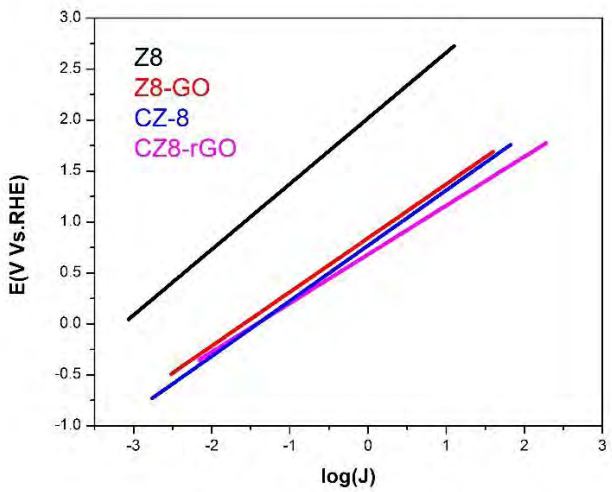

Figure.3.26 Tafel slope of ZIF-8 for OER

In these graphs, C-ZIF-8/rGO shows the least tafel slope of -79 $mVdec^{-1}$ for HER and -75 $mVdec^{-1}$ for OER.

Table 3.8 Tafel slope results of ZIF-8 for HER

Material	**Tafel slope ($mVdec^{-1}$)**
ZIF-8	**-142**
ZIF-8/GO	**-129**
C-ZIF-8	**-112**
C-ZIF-8/rGO	**-79**

Table.3.9. Tafel slope results of ZIF-8 for OER

Materials	Tafel slope (mV/dec)
ZIF-8	-133
ZIF-8/GO	-120
C-ZIF-8	-104
C-ZIF-8/rGO	-75

Conclusions

Noble metals (particularly Pt/Pd) based electrocatalysts have high action towards HER and OER yet their significant expense and shortage restricts thir application. Therefore an exertion was made to synthesize good electrocatalyst for HER and OER that can be an option for precious metal (Pt/Pd) based electrocatalysts. In such manner, Co and Zn based ZIFs (subclass of MOFs) have practically compareable activity with that of noble metals due to their multi-electron transfer reaction, better strength and simple accessibility. To expand the conductivity and electrocatalytic action of the material, composite of ZIF-67 and ZIF-8 were made with GO followed by their carbonization that further upgrades their electrical conductivity and they displays great chemical and mechanical strength.

Simple mixing method (stirring and sonication) was used to synthesize ZIF-67, ZIF-8, ZIF-8/GO and ZIF-67/GO followed by their carbonization in tube furnace. The synthesized materials were characterized and analyzed by XRD, IR, TGA, and SEM, BET and EDX. XRD confirms the purity and crystallinity of material. IR confirms the presence of functional groups. Similarly TGA and BET gives the information about the thermal stability and surface area of the material. All these characterization ensures the synthesis of our material. Electrochemical studies of the synthezied material were done by using linear sweep voltammetry (LSV) and electrochemical impedence spectroscopy (EIS). ZIF-67 and ZIF-8 are prefered because of simplicity of synthesis, low cost precursors and existence of highly electroconductive Zn or Co metals that promotes the electron/mass transfer during the reaction. After the considerations and deep analysis of characterization and electrochemical studies, it was concluded that carbonized ZIF-67/rGO showed the maximum current density of 130mAcm^{-2} for HER and 140mAcm^{-2} for OER while carbonized ZIF-8/rGO showed the maximum current density of 170mAcm^{-2} for HER and 190mAcm^{-2} for OER due to their high surface area, good electrical conductivity and excellent mechanical strength.

References

1. Su, D. S.; Schlögl, R., Nanostructured carbon and carbon nanocomposites for electrochemical energy storage applications. *ChemSusChem: Chemistry & Sustainability Energy & Materials* **2010,** *3* (2), 136-168.

2. Chang, Z.; Huo, S.; Zhang, W.; Fang, J.; Wang, H., The tunable and highly selective reduction products on Ag@ Cu bimetallic catalysts toward CO2 electrochemical reduction reaction. *J. Phys. Chem. C.* **2017,** *121* (21), 11368-11379.

3. Mekhilef, S.; Saidur, R.; Safari, A., Comparative study of different fuel cell technologies. *Renewable Sustainable Energy Rev.* **2012,** *16* (1), 981-989.

4. Wu, A.; Xie, Y.; Ma, H.; Tian, C.; Gu, Y.; Yan, H.; Zhang, X.; Yang, G.; Fu, H., Integrating the active OER and HER components as the heterostructures for the efficient overall water splitting. *Nano Energy* **2018,** *44*, 353-363.

5. i Xamena, F. X. L.; Abad, A.; Corma, A.; Garcia, H., MOFs as catalysts: Activity, reusability and shape-selectivity of a Pd-containing MOF. *J. Catal.* **2007,** *250* (2), 294-298.

6. Nik, O. G.; Chen, X. Y.; Kaliaguine, S., Functionalized metal organic framework-polyimide mixed matrix membranes for CO2/CH4 separation. *J. Membr. Sci.* **2012,** *413*, 48-61.

7. Stock, N.; Biswas, S., Synthesis of metal-organic frameworks (MOFs): routes to various MOF topologies, morphologies, and composites. *Chem. Rev.* **2012,** *112* (2), 933-969.

8. Khan, N. A.; Jhung, S. H., Synthesis of metal-organic frameworks (MOFs) with microwave or ultrasound: Rapid reaction, phase-selectivity, and size reduction. *Coord. Chem. Rev.* **2015,** *285*, 11-23.

9. Son, W.-J.; Kim, J.; Kim, J.; Ahn, W.-S., Sonochemical synthesis of MOF-5. *Chem. Commun.* **2008,** (47), 6336-6338.

10. de Lima Neto, O. J.; de Oliveira Frós, A. C.; Barros, B. S.; de Farias Monteiro, A. F.; Kulesza, J., Rapid and efficient electrochemical synthesis of a zinc-based nano-MOF for Ibuprofen adsorption. *New. J. Chem.* **2019,** *43* (14), 5518-5524.

11. Lv, D.; Chen, Y.; Li, Y.; Shi, R.; Wu, H.; Sun, X.; Xiao, J.; Xi, H.; Xia, Q.; Li, Z., Efficient mechanochemical synthesis of MOF-5 for linear alkanes adsorption. *J. Chem. Eng. Data* **2017,** *62* (7), 2030-2036.

12. (a) Esken, D.; Turner, S.; Lebedev, O. I.; Van Tendeloo, G.; Fischer, R. A., Au@ ZIFs: stabilization and encapsulation of cavity-size matching gold clusters inside functionalized zeolite imidazolate frameworks, ZIFs. *Chem. Mater.* **2010,** *22* (23), 6393-6401; (b) Bhattacharjee, S.; Jang, M.-S.; Kwon, H.-J.; Ahn, W.-S., Zeolitic imidazolate frameworks: synthesis, functionalization, and catalytic/adsorption applications. *Catal. Surv. Asia* **2014,** *18* (4), 101-127.

13. Chul, H. D.; Vinodh, R.; Gopi, C. V. M.; Deviprasath, C.; Kim, H.-J.; Yi, M., Effect of the cobalt and zinc ratio on the preparation of zeolitic imidazole frameworks (ZIFs): synthesis, characterization and supercapacitor applications. *Dalton Trans.* **2019,** *48* (39), 14808-14819.

14. Chen, B.; Yang, Z.; Zhu, Y.; Xia, Y., Zeolitic imidazolate framework materials: recent progress in synthesis and applications. *J. Mater. Chem. A.* **2014,** *2* (40), 16811-16831.

15. Imawaka, K.; Sugita, M.; Takewaki, T.; Tanaka, S., Mechanochemical synthesis of bimetallic CoZn-ZIFs with sodalite structure. *Polyhedron* **2019,** *158*, 290-295.

16. Durst, J.; Siebel, A.; Simon, C.; Hasche, F.; Herranz, J.; Gasteiger, H., New insights into the electrochemical hydrogen oxidation and evolution reaction mechanism. *Energy Environ. Sci.* **2014,** *7* (7), 2255-2260.

17. Chun, J. H.; Jeon, S. K.; Kim, B. K.; Chun, J. Y., Determination of the Langmuir adsorption isotherms of under-and over-potentially deposited hydrogen for the cathodic H2 evolution reaction at poly-Ir/aqueous electrolyte interfaces using the phase-shift method. *Int. J. Hydrogen Energy* **2005,** *30* (3), 247-259.

18. Chang, L.; Cheng, D.; Sementa, L.; Fortunelli, A., Hydrogen evolution reaction (HER) on Au@ Ag ultrananoclusters as electro-catalysts. *Nanoscale* **2018,** *10* (37), 17730-17737.

19. Tilak, B.; Chen, C.-P., Generalized analytical expressions for Tafel slope, reaction order and ac impedance for the hydrogen evolution reaction (HER): mechanism of HER on platinum in alkaline media. *J. Appl. Electrochem.* **1993,** *23* (6), 631-640.

20. Reier, T.; Oezaslan, M.; Strasser, P., Electrocatalytic oxygen evolution reaction (OER) on Ru, Ir, and Pt catalysts: a comparative study of nanoparticles and bulk materials. *ACS Catal.* **2012,** *2* (8), 1765-1772.

21. Kibria, A. F.; Tarafdar, S., Electrochemical studies of a nickel–copper electrode for the oxygen evolution reaction (OER). *Int. J. Hydrogen Energy* **2002,** *27* (9), 879-884.

22. Curutchet, A.; Colinet, P.; Michel, C.; Steinmann, S. N.; Le Bahers, T., Two-sites are better than one: revisiting the OER mechanism on CoOOH by DFT with electrode polarization. *Phys. Chem. Chem. Phys.* **2020,** *22* (13), 7031-7038.

23. Shi, Q.; Zhu, C.; Du, D.; Lin, Y., Robust noble metal-based electrocatalysts for oxygen evolution reaction. *Chem. Soc. Rev.* **2019,** *48* (12), 3181-3192.

24. Yuan, N.; Jiang, Q.; Li, J.; Tang, J., A review on non-noble metal based electrocatalysis for the oxygen evolution reaction. *Arabian J. Chem.* **2020,** *13* (2), 4294-4309.

25. Braz, C. E. M.; Crnkovic, P. C. G. M., Physical-chemical characterization of biomass samples for application iin pyrolysis process. *Chem. Eng. Trans.* **2014**, 523-528.

26. Demirbas, A.; Arin, G., An overview of biomass pyrolysis. *Energy sources* **2002,** *24* (5), 471-482.

27. Guo, H.; Jia, W.; Zeng, J.; He, R., Evolution of organic matter and nanometer-scale pores in an artificially matured shale undergoing two distinct types of pyrolysis: A study of the Yanchang Shale with Type II kerogen. *Org. Geochem.* **2017,** *105*, 56-66.

28. Guizani, C.; Jeguirim, M.; Valin, S.; Limousy, L.; Salvador, S., Biomass chars: The effects of pyrolysis conditions on their morphology, structure, chemical properties and reactivity. *Energies* **2017,** *10* (6), 796.

29. Kidena, K.; Murata, S.; Nomura, M., Studies on the chemical structural change during carbonization process. *Energy Fuels* **1996,** *10* (3), 672-678.

30. Wang, J.; Fan, Y.; Qi, S.; Li, W.; Zhao, M., Bifunctional HER/OER or OER/ORR catalytic activity of two-dimensional TM3 (HITP) 2 with TM= Fe–Zn. *The J. Phy. Chem. C.* **2020,** *124* (17), 9350-9359.

31. Zhu, L.; Liu, X.-Q.; Jiang, H.-L.; Sun, L.-B., Metal–organic frameworks for heterogeneous basic catalysis. *Chem. Rev.* **2017,** *117* (12), 8129-8176.

32. Zanon, A.; Verpoort, F., Metals@ ZIFs: Catalytic applications and size selective catalysis. *Coord. Chem. Rev.* **2017,** *353*, 201-222.

33. Chen, B.; Zhu, Y.; Xia, Y., Controlled in situ synthesis of graphene oxide/zeolitic imidazolate framework composites with enhanced CO 2 uptake capacity. *RSC Adv.* **2015,** *5* (39), 30464-30471.

34. Cullity, B. D., *Elements of X-ray Diffraction*. Addison-Wesley Publishing: 1956.

35. Berthomieu, C.; Hienerwadel, R., Fourier transform infrared (FTIR) spectroscopy. *Photosynth. Res.* **2009,** *101* (2), 157-170.

36. Prime, R. B.; Bair, H. E.; Vyazovkin, S.; Gallagher, P. K.; Riga, A., Thermogravimetric analysis (TGA). *Thermal analysis of polymers: Fundamentals and applications. J. Therm. Anal. Calorim.* **2009**, 241-317.

37. Zhou, W.; Apkarian, R.; Wang, Z. L.; Joy, D., Fundamentals of scanning electron microscopy (SEM). *J. Nanotechnol.* Springer: 2006; pp 1-40.

38. Scimeca, M.; Bischetti, S.; Lamsira, H. K.; Bonfiglio, R.; Bonanno, E., Energy Dispersive X-ray (EDX) microanalysis: A powerful tool in biomedical research and diagnosis. *Eur. J. Histochem: EJH* **2018,** *62* (1).

39. Marcano, D. C.; Kosynkin, D. V.; Berlin, J. M.; Sinitskii, A.; Sun, Z.; Slesarev, A.; Alemany, L. B.; Lu, W.; Tour, J. M., Improved synthesis of graphene oxide. *ACS nano* **2010,** *4* (8), 4806-4814.

40. Lin, K.-Y. A.; Chang, H.-A., Ultra-high adsorption capacity of zeolitic imidazole framework-67 (ZIF-67) for removal of malachite green from water. *Chemosphere* **2015,** *139*, 624-631.

41. Lashgari, S. M.; Yari, H.; Mahdavian, M.; Ramezanzadeh, B.; Bahlakeh, G.; Ramezanzadeh, M., Synthesis of graphene oxide nanosheets decorated by nanoporous zeolite-imidazole (ZIF-67) based metal-organic framework with controlled-release corrosion inhibitor performance: Experimental and detailed DFT-D theoretical explorations. *J. Hazard. Mater.* **2021,** *404*, 124068.

42. Guo, Y.; Tang, J.; Salunkhe, R. R.; Alothman, Z. A.; Hossain, M. S. A.; Malgras, V.; Yamauchi, Y., Effect of various carbonization temperatures on ZIF-67 derived nanoporous carbons. *Bull. Chem. Soc. Jpn.* **2017,** *90* (8), 939-942.

43. Lee, Y.-R.; Jang, M.-S.; Cho, H.-Y.; Kwon, H.-J.; Kim, S.; Ahn, W.-S., ZIF-8: A comparison of synthesis methods. *Chem. Eng. J.* **2015,** *271*, 276-280.

44. Kim, D.; Kim, D. W.; Hong, W. G.; Coskun, A., Graphene/ZIF-8 composites with tunable hierarchical porosity and electrical conductivity. *J. Mater. Chem. A.* **2016,** *4* (20), 7710-7717.

45. Yuan, Y.; Xu, X.; Xia, J.; Zhang, F.; Wang, Z.; Liu, Q., A hybrid material composed of reduced graphene oxide and porous carbon prepared by carbonization of a zeolitic imidazolate framework (type ZIF-8) for voltammetric determination of chloramphenicol. *Microchim. Acta* **2019,** *186* (3), 1-8.

46. Shahrak, M. N.; Ghahramaninezhad, M.; Eydifarash, M., Zeolitic imidazolate framework-8 for efficient adsorption and removal of Cr (VI) ions from aqueous solution. *Environ. Sci. Pollut. Res.* **2017,** *24* (10), 9624-9634.

47. Zhou, K.; Mousavi, B.; Luo, Z.; Phatanasri, S.; Chaemchuen, S.; Verpoort, F., Characterization and properties of Zn/Co zeolitic imidazolate frameworks vs. ZIF-8 and ZIF-67. *J. Mater. Chem. A.* **2017,** *5* (3), 952-957.

48. Ding, H.; Zhang, X.-K.; Fan, J.-Q.; Zhan, X.-q.; Xie, L.; Shi, D.; Jiang, T.; Tsai, F.-C., MOF-templated synthesis of Co3O4@ TiO2 hollow dodecahedrons for high-storage-density lithium-ion batteries. *ACS omega* **2019,** *4* (8), 13241-13249.

49. Pan, Y.; Liu, Y.; Zeng, G.; Zhao, L.; Lai, Z., Rapid synthesis of zeolitic imidazolate framework-8 (ZIF-8) nanocrystals in an aqueous system. *Chem. Commun.* **2011,** *47* (7), 2071-2073.

50. Shahriary, L.; Athawale, A. A., Graphene oxide synthesized by using modified hummers approach. *Int. J. Renew. Energy Environ. Eng* **2014,** *2* (01), 58-63.

51. Zhu, Q.; Zhuang, W.; Chen, Y.; Wang, Z.; Villacorta Hernandez, B.; Wu, J.; Yang, P.; Liu, D.; Zhu, C.; Ying, H., Nano-biocatalysts of Cyt c@ ZIF-8/GO composites with high recyclability via a de novo approach. *ACS Appl. Mater. Interfaces* **2018,** *10* (18), 16066-16076.

52. Mermoux, M.; Chabre, Y.; Rousseau, A., FTIR and 13C NMR study of graphite oxide. *Carbon* **1991,** *29* (3), 469-474.

53. Archana, K.; Pillai, N. G.; Rhee, K. Y.; Asif, A., Super paramagnetic ZIF-67 metal organic framework nanocomposite. *Composites Part B: Engineering* **2019,** *158*, 384-389.

54. Hu, G.; Zhang, W.; Chen, Y.; Xu, C.; Liu, R.; Han, Z., Removal of boron from water by GO/ZIF-67 hybrid material adsorption. *Environ. Sci. Pollut. Res.* **2020,** *27* (22), 28396-28407.

55. Guo, J.; Gadipelli, S.; Yang, Y.; Li, Z.; Lu, Y.; Brett, D. J.; Guo, Z., An efficient carbon-based ORR catalyst from low-temperature etching of ZIF-67 with ultra-small cobalt nanoparticles and high yield. *J. Mater. Chem.A.* **2019,** *7* (8), 3544-3551.

56. Hu, Y.; Kazemian, H.; Rohani, S.; Huang, Y.; Song, Y., In situ high pressure study of ZIF-8 by FTIR spectroscopy. *Chem. Commun.* **2011,** *47* (47), 12694-12696.

57. Zhang, M.; Shi, X.; Dai, X.; Huo, C.; Xie, J.; Li, X.; Wang, X., Improving the crystallization and fire resistance of poly (lactic acid) with nano-ZIF-8@ GO. *J. Mater. Sci.* **2018,** *53* (9), 7083-7093.

58. Wang, L.; Wang, C.; Wang, H.; Jiao, X.; Ouyang, Y.; Xia, X.; Lei, W.; Hao, Q., ZIF-8 nanocrystals derived N-doped carbon decorated graphene sheets for symmetric supercapacitors. *Electrochim. Acta* **2018,** *289*, 494-502.